

**SELECTION OF MATERIAL FOR DEEP DRAWING OF A FUEL TANK AND ITS  
FINITE ELEMENT SIMULATION**

A THESIS SUBMITTED IN PARTIAL FULFILLMENT OF THE REQUIREMENT FOR  
THE AWARD OF THE DEGREE OF

**MASTER OF TECHNOLOGY**

(COMPUTATIONAL DESIGN)

TO

**DELHI TECHNOLOGICAL UNIVERSITY**



SUBMITTED BY

**SUNIL KUMAR**

**ROLL NO.:2K15/CDN/14**

UNDER THE GUIDANCE OF

**DR. VIJAY GAUTAM**

**ASST. PROFESSOR**

DELHI TECHNOLOGICAL UNIVERSITY

**DEPARTMENT OF MECHANICAL, PRODUCTION & INDUSTRIAL AND  
AUTOMOBILE ENGINEERING**

**DELHI TECHNOLOGICAL UNIVERSITY**

**BAWANA ROAD, DELHI-110042**



**BAWANA ROAD, DELHI-110042**

**DELHI TECHNOLOGICAL  
UNIVERSITY**

(Formerly Delhi college of Engineering)

Shahbad Daulatpur, Baawana Road,

Delhi-110042

---

### **STUDENT'S DECLARATION**

I, **Sunil Kumar**, hereby certify that the work which is being presented in this thesis titled “**Selection of Material for Deep Drawing of a Fuel Tank And Its Finite Element Simulation**” is submitted in the partial fulfilment of the requirement for degree of **Master of Technology (Computational Design)** in Department of Mechanical Engineering at **Delhi Technological University** is an authentic record of my own work carried out under the supervision of **Dr. Vijay Gautam**. The matter presented in this thesis has not been submitted in any other University/Institute for the award of Master of Technology Degree. Also, it has not been directly copied from any source without giving its proper reference.

#### **Signature of Student**

This is to certify that the above statement made by the candidate is correct to the best of my knowledge.

#### **Signature of Supervisor**



Delhi-110042

**DELHI TECHNOLOGICAL UNIVERSITY**

(Formerly Delhi college of Engineering)

Shahbad Daulatpur, Bawana Road,

---

### **CERTIFICATE**

This is to certify that this thesis report titled, **“Selection of Material for Deep Drawing of a Fuel Tank And Its Finite Element Simulation”** being submitted by **Sunil Kumar (Roll No. 2K15/CDN/14)** at Delhi Technological University, Delhi for the award of the Degree of Master of Technology as per academic curriculum. It is a record of bonafide research work carried out by the student under my supervision and guidance, towards partial fulfilment of the requirement for the award of Master of Technology degree in Computational Design. The work is original as it has not been submitted earlier in part or full for any purpose before.

**Dr. Vijay Gautam**

**Asst. Professor**

**Mechanical Engineering Department**

**Delhi Technological University**

**Delhi-110042**

## ACKNOWLEDGEMENT

First and foremost, praises and thanks to the God, the Almighty, for His showers of blessings throughout my research work to complete the research successfully.

I would like to extend my gratitude to **Prof. R.S. Mishra, Head,** Department of Mechanical Engineering, Delhi Technological University, for providing this opportunity to carry out the present thesis work.

The constant guidance and encouragement received from **Dr. A.K. Agarwal, M.Tech. Coordinator and Associate Professor,** Department of Mechanical Engineering, Delhi Technological University, has been of great help in carrying out the present work and is acknowledge with reverential thanks.

I would like to express my deep and sincere gratitude to my research supervisor, **Dr. Vijay Gautam,** Department of Mechanical Engineering, Delhi Technological University, for giving me the opportunity to do research and providing invaluable guidance throughout this research. His dynamism, vision, sincerity and motivation have deeply inspired me. He has taught me the methodology to carry out the research and to present the research works as clearly as possible. It was a great privilege and honour to work and study under his guidance. I am extremely grateful for what he has offered me. I would like to thanks him for his friendship, empathy, and great sense of humour. Without the wise advice and able guidance, it would have been impossible to complete the thesis in this manner.

I am extremely grateful to my parents and family for their love, prayers, caring and sacrifices for educating and preparing me for the future.

**SUNIL KUMAR**

**M.Tech (COMPUTATIONAL DESIGN)**

**2K15/CDN/14**

## **ABSTRACT**

Deep drawing is a sheet metal forming process in which deformation forces are oriented in the plane of the sheet, and the surface pressures in the tool are generally lower than the yield stress of the sheet material. The limits of the sheet metal forming are determined by the occurrence of defects such as wrinkling and tearing on the blank which are the most frequent types of failure. The present work discusses the numerical investigations of deep drawing of a cold rolled draw quality steel and interstitial free steel blank of 0.8mm and 1.2mm thickness in to a shape of a fuel tank with varying blank holding forces. The tensile specimens are laser cut from a blank with known rolling direction as per ASTM E8M standard and are tested for tensile properties and anisotropy. These properties were used in the material model in FE analysis of the process using HYPERWORKS. It is observed numerically that optimum blank holder force is necessary to remove the wrinkling defects. Deep drawing parameters like percentage thinning and plastic strain along with respective forming limit diagrams have been obtained for individual cases and thus changes in these parameters with varying thickness and material is area of investigation for understanding deep drawing process over fuel tank.

Keywords: Deep drawing, yield stress, cold rolled draw quality, Interstitial Free Steel, blank holding force, FE analysis, HYPERWORKS.

## Contents

STUDENT DECLARATION	i
CERTIFICATE	ii
ACKNOWLEDGEMENT	iii
ABSTRACT	iv
CHAPTER 1	6
INTRODUCTION	6
1.1 Sheet Metal Forming	6
1.2 Plastic Deformation in Sheet Metal Forming	8
1.3 Deep Drawing	10
1.3.1 Introduction	10
1.3.2 Stages in deep drawing	11
1.3.3 Stresses in deep drawing	12
1.3.4 Material Deformation in Deep Drawing	14
1.3.5 Formability of the Sheets	15
1.3.5.1 Formability Tests	15
1.3.5.1.1 Erichsen Test	15
1.3.5.1.2 Swift's Cup Test	16
1.3.5.1.3 Fukui Test	17
1.3.5.2 Forming Limit Diagram	18
1.3.6 Limiting Drawing Ratio	19
1.3.6.1 Redrawing	20
1.3.7 Factors Affecting Deformation Deep Drawing	20
1.3.7.1 Design Parameters	21
1.3.7.1.1 Die Corner Radius	21
1.3.7.1.2 Punch Corner Radius	21
1.3.7.1.3 Radial Clearance	22
1.3.7.1.4 Blank Thickness	23
1.3.7.2 Material Parameters	23
1.3.5.2.1 Anisotropy	23

1.3.7.2.2 Strength Co-efficient	24
1.3.7.2.3 Work Hardening Co-efficient	24
1.3.7.3 Process Parameters	25
1.3.7.3.1 Blank Holding Force	25
1.3.7.3.2 Friction	26
1.3.7.3.3 Punch Velocity	28
1.3.8 Defects in Deep Drawing	29
1.5 Objective	31
1.6 Organization of Thesis	32
CHAPTER 2	33
LITERATURE REVIEW	33
CHAPTER 3	45
MODELING & SIMULATION	45
3.1 Modeling	45
3.2 Simulation	46
3.2.1 Radioss One-Step Analysis	47
3.2.2 Die Module	47
3.2.3 Incremental Forming	47
CHAPTER 4	53
EXPERIMENTAL WORK	53
4.1 Materials Selection	53
4.1.1 Interstitial Free steel	54
4.1.2 Cold Rolled Deep Quality	54
4.2 Determination of tensile properties	55
4.3 Mechanical Properties of Materials	57
CHAPTER 5	61
RESULTS AND DISCUSSION	61
CHAPTER 6	74
CONCLUSION AND FUTURE SCOPE	74
6.1 Conclusion	74
6.2 Future Scope	74

## List of Tables

Table 1.1 Modes of deformation	9
Table 3.1 Friction values	52
Table 4.1: Chemical composition of the CRDQ & IF steel used (by weight %)	53
Table 4.2: Different Mechanical properties of CRDQ & IF steel	58



## List of figures

Fig. 1.1 Bulk Deformation Processes	7
Fig.1.2 Sheet-metal-forming processes.	7
Fig.1.3 Various State of Stress on Strain Plane	8
Fig. 1.4 Geometry of drawing die assembly with circular blank	10
Fig 1.5 stages in the deep drawing process	12
Fig. 1.6 State of stress in different zones of deep drawn cup.	13
Fig.1.7 Erichsen Test	16
Fig. 1.8 Swift's Cup Test	17
Fig. 1.9 Fukui Test	17
Fig. 1.10 Forming limit curve showing different strain combinations responsible for failure.	18
Fig. 1.11 FLC for the low and high values of work-hardening co-efficient	19
Fig. 1.13 Graph showing variation of draw depth w.r.t blank holding force	26
Fig.1.14 Friction regions in a deep drawing a cup. (A) Friction surface between blank and binder & die; (B) friction surface between blank & the die corner radius and (C) friction surface between blank & the punch corner radius; $F_p$ , total drawing force; $F_H$ , blank holding force.	28
Fig. 1.15 Earing defect w.r.t rolling direction	30
Fig. 1.16 Various failure modes in deep-drawing	31
Fig.2.1: Strains on a tensile-test specimen removed from a piece of sheet metal.	34
Fig.2.2: Punch load/travel diagrams for all materials drawn with (a) smooth punch (b)rough punch	36
Fig.2.3: (a) Schematic diagram of five regions in the deep drawing by an elliptical punch. (b)Schematic diagram of five regions in the deep drawing by a clover-type punch.	37
Fig.2.4: Adaptively redesigned meshes for the test part example	38
Fig.2.5: Forming limit diagram defined by Keeler	39
Fig.2.6: Forming limit diagrams defined by Keeler and Goodwin	40
Fig.2.7: Forming limit diagrams for necking and for fracture	41
Fig. 3.1 Die Face Designed in Die Module	45
Fig. 3.2 Blank	46
Fig. 3.3 Die with meshing	48
Fig. 3.4 Punch	49
Fig. 3.5 (A) Binder (B) Blank	50
Fig. 3.6 From upside (1) Die (2) Blank (3) Binder (4 )Punch	51
Fig. 4.1: Dimensions of Tensile specimen (ASTM E8)	55
Fig. 4.2 50kN-UTM-table top in Metal Forming Lab. at DTU	56
Fig. 4.3 Tensile test specimens in $0^\circ$ , $45^\circ$ and $90^\circ$ to rolling direction as per ASTM E8M standard.	56
Fig. 4.4 Engineering Stress-Strain Curve of CRDQ Steel	58
Fig. 4.5 True Stress-strain curve CRDQ Steel	59
Fig. 4.6 Engineering stress (MPa)-strain curve of IF Steel	59

Fig. 4.7 True stress (MPa) – strain curve IF Steel	60
Figure 5.1 An incomplete draw part under 25 KN binder force.	61
Fig. 5.2 (A) Variation of the thickness throughout the blank. (B) Percentage thinning contour of 0.8mm	62
Fig. 5.4 Forming limit diagram of the 0.8 mm thick IF Steel blank.	64
Fig. 5.5 (A) Contour plot of the variation of the scalar value of thickness 1.2 mm thick blank. (B) Percentage thinning contour plot of 1.2 mm thick IF Steel blank.	66
Fig.5.7 FLD of the 1.2mm thick IF Steel blank.	68
Fig. 5.8 Percentage Thinning 0.8mm CRDQ Steel Blank	68
Fig. 5.9 Plastic Strain 0.8mm CRDQ Steel	69
Fig. 5.10 Forming Limit Diagram 0.8 mm thick CRDQ Steel Blank	70
Fig. 5.11 Percentage thinning of 1.2mm thick CRDQ Steel Blank	71
Fig. 5.12 Plastic strain 1.2mm CRDQ Steel	71
Fig. 5.13 FLD 1.2mm thick CRDQ Steel Blank	72

# CHAPTER 1

## INTRODUCTION

### 1.1 Sheet Metal Forming

Sheet metal components are used in a major variety of applications in the industries, with finding much of its use in automobile, aerospace, packaging (beverages can, food containers) and home appliances industry. Before the industrial use most of the metals first processed to form ingots and slabs which are further processed to make the different kind of semi finished products for the different metal forming processes.

Metal forming includes a broad range of industrialized processes in which the metal work-piece undergoes a plastic change in the profile by the application of external forces by means of a variety of forming tools. It is extremely important to differentiate between the terms “deforming” and “forming”. In the case of unrestrained plastic straining, the term “deforming” should be used whereas the term “forming” should be used with proscribed plastic strain to gain a specific profile for the part.

Metal forming processes are categorized into bulk deformation processes and sheet metal forming processes, where the former refers to the category of processes that change the shape/size of the work-piece extensively, and the latter refers to the category of processes performed on metallic sheets, whose thickness lies in the range of 0.4mm to 6mm. Unlike the bulk forming processes, the major characteristic of sheet metal forming is the use of a work-piece with high ratio of surface area to thickness. In sheet metal forming, tensile forces are mainly utilized in the plane of the sheet to achieve the process, whereas compressive forces that are generated in the transverse direction as a result of the tension may result in folding or wrinkling of the sheet. As a result, any reduction in the thickness is due to tensile stress induced in the sheet itself. Therefore, the most important concern in all sheet metal forming processes is to avoid excessive decreasing in thickness, which can lead to necking and

fracture. Usually most of the sheets forming processes are carried out at room temperature (cold processing conditions) excepting if the work piece is thick; the sheet metal is brittle or the deformation is massive.

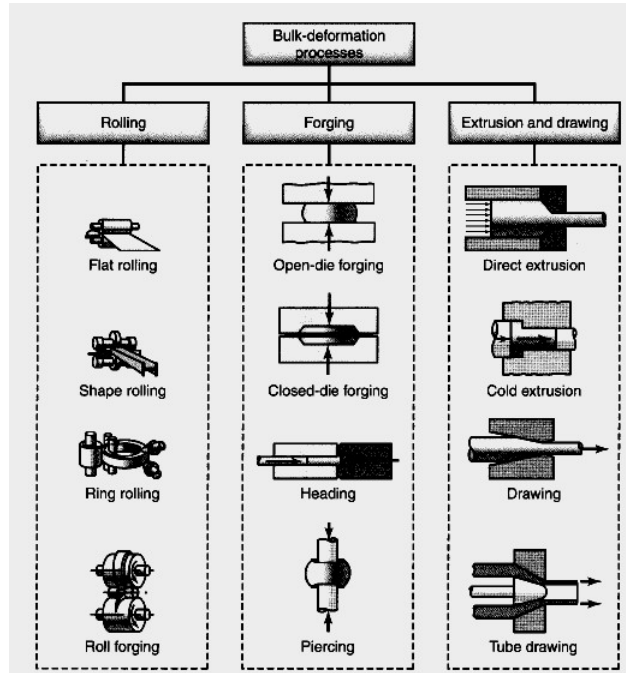


Fig. 1.1 Bulk Deformation Processes

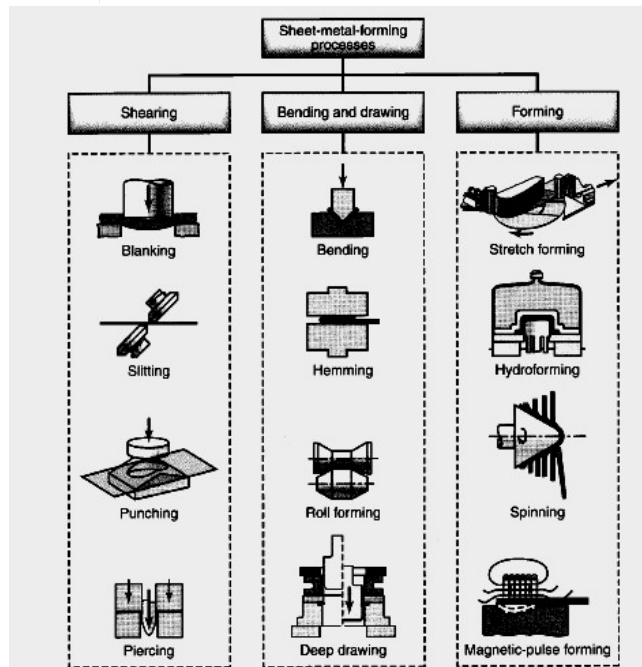


Fig.1.2 Sheet-metal-forming processes.

## 1.2 Plastic Deformation in Sheet Metal Forming

The analysis of the deformation mechanism in sheet metal forming is based on the two principal strains  $\epsilon_1$  and  $\epsilon_2$ . Mostly, the maximum principal strain  $\epsilon_1$  is positive in forming operations, so only half of the strain plane is considered as shown in the figure 1.3 & 1.4. Deformation pairs relative to different points of a stamped part are often plotted on such a half-plane. This information can be drawn either from FE simulation or from experimental analysis (grids). The study of such deformation plots gives useful insights into the mechanics of a forming process.

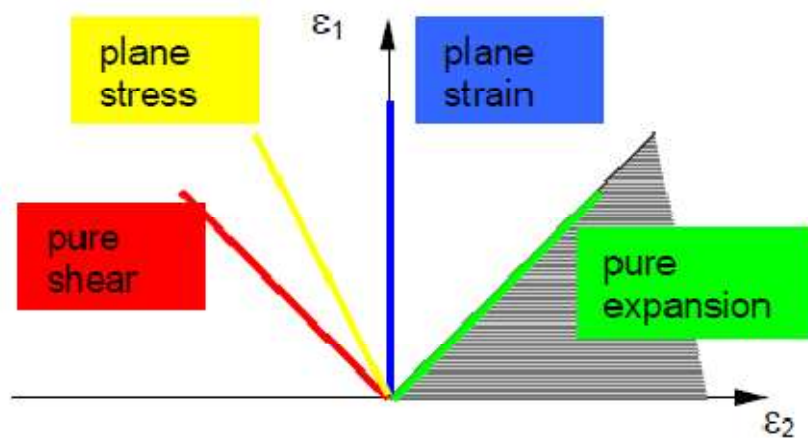
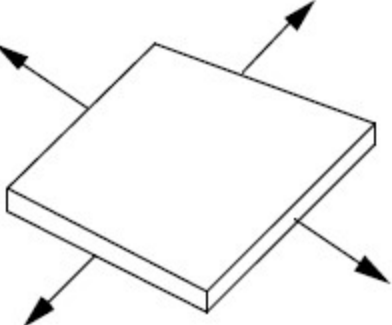
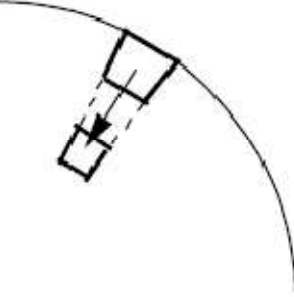




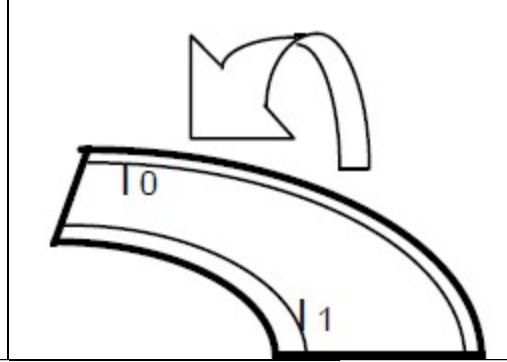
Fig.1.3 Various State of Stress on Strain Plane. [36]

In this section various deformation modes which take place in the sheet metal forming is discussed. In sheet metal forming, we have five basic modes of deformation:

Table 1.1 Modes of deformation

<p><b>STRETCHING:</b> The material is expanded in both directions. This mode of deformation is found mostly on smooth bottoms of shallow parts and in hydroforming processes.</p>	
<p><b>DRAWING:</b> This mode is typical the material flow from the flange towards the inner part of the die.</p>	
<p><b>BENDING/UNBENDING:</b> This is a cyclic deformation (most often associated with plane strain). It is found on the die entry line as well as in drawbeads.</p>	
<p><b>STRETCH-AND-BEND:</b> This mode is associated to flanging operations for which the bending line is concave.</p>	

COMPRESSION-AND-BEND: This mode is associated to flanging operations for which the bending line is convex.



### 1.3 Deep Drawing

#### 1.3.1 Introduction

Deep drawing is one of the mostly used processes in the sheet metal forming industries. In this process a flat blank is shaped into metal is squeezed between the punch and die to get the desire shape and simultaneously the blank holding force is also applied on the blank. The shape of the product manufactured by the deep drawing can be symmetric or asymmetric depending upon the application. Containers, automobile parts, such as fuel tank and panels, pans, cans and cooking appliances are among the wide variety of the products manufactured by the deep drawing process. The basic mechanism and different elements of a deep drawing process is shown in the figure (1.4).

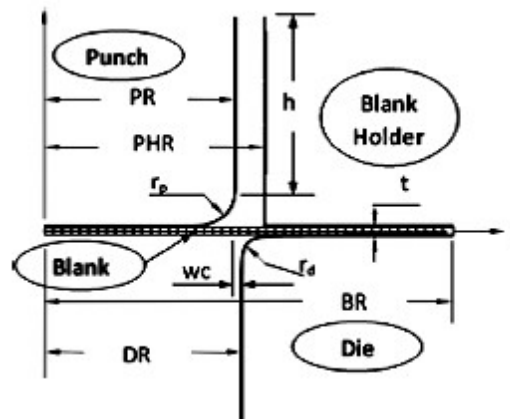


Fig. 1.4 Geometry of drawing die assembly with circular blank [1]

Generally, a binding or hold-down pressure is required to press the blank against the die to prevent wrinkling. The best way to do this in a double-action is by using of a binder or blank holder. The basic variables in deep drawing process are punch radius, PR; die radius, DR; blank radius, BR; thickness of blank, t; punch corner radius,  $r_p$ ; die corner radius,  $r_d$ ; radial clearance between die and punch, wc; friction co-efficient between the contacting surfaces like between die & blank, punch & blank and binder & blank; properties of the material to be drawn.

The material flow and force distribution involved in the deep drawing is very complex. There are two major factors which helps in drawing of a component, rather than shearing it. These are die corner radius and punch corner radius. A radius on an edge will change the force distribution and cause the metal to flow over the radius and into the die cavity. However, there are changes in thickness in certain areas, due to the forces involved. Material forming the straight wall is under tensile stress that will naturally cause it to thin. Deep drawing process factors are controlled to mitigate thinning, but some thinning of the sheet metal is inevitable. Maximum thinning will most likely occur on the side wall, near the base of the part. A correctly drawn part may have up to 25% reduction in thickness in some areas [1].

### **1.3.2 Stages in deep drawing**

The process of deep drawing can be divided into five different stages as shown in the figure (1.5)

- I. Punch makes initial contact with blank
- II. Bending
- III. Straightening
- IV. Friction and compression
- V. Final cup shape showing effects of thinning in the cup walls



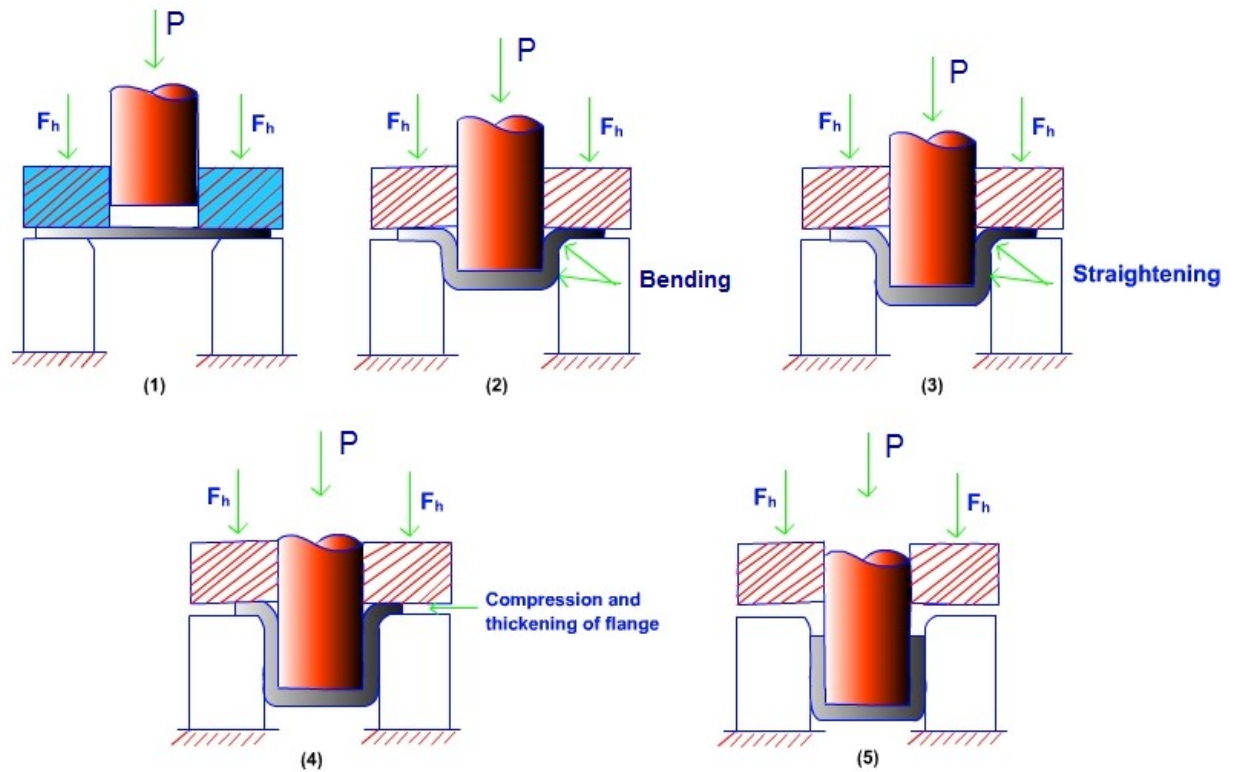


Fig 1.5 stages in the deep drawing process

In the first stage the punch comes in contact with blank, pushes the blank into the die cavity, and the holding plate applies a holding force on the blank. The flat portion of the sheet under the holding plate moves towards the die axis, then bends over the die profile. After bending over the die profile, the sheet unbends to flow downward along the side wall. The vertical portion of the sheet then slips past the die surface. More metal is drawn towards the center of the die to replace the metal that has already flowed into the die wall. Friction between the holding plate and blank and that between the die and blank must be overcome by the blank during the horizontal flow of metal.

### 1.3.3 Stresses in deep drawing

Any deep drawn part is divided into three major regions on the basis of stress, namely the punch region, wall region, and flange region as shown in the figure 1.8.

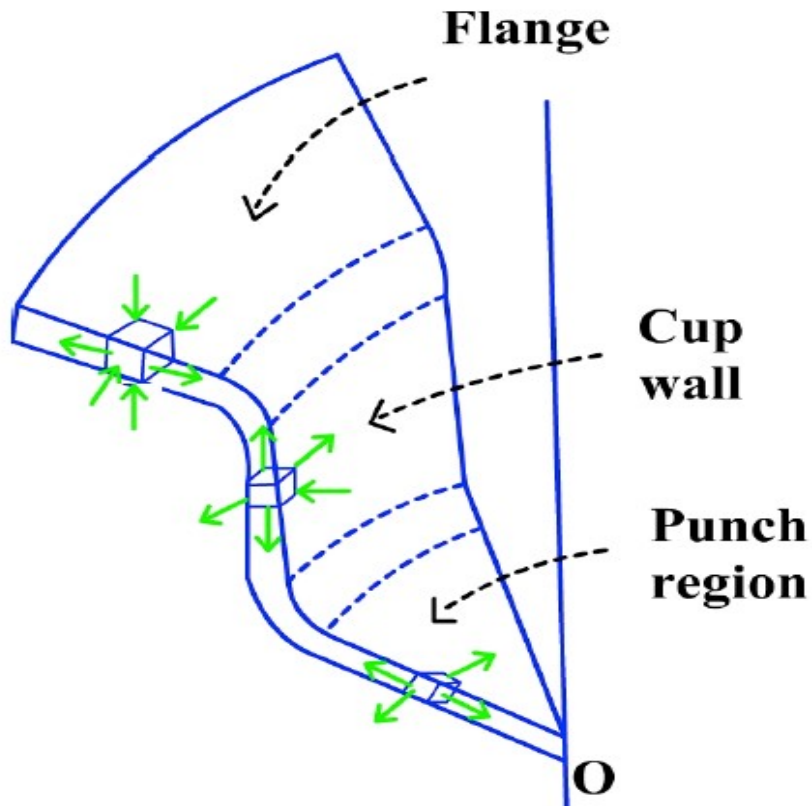


Fig. 1.6 State of stress in different zones of deep drawn cup.

- **Punch Region:** The area of the blank which is in contact with the punch undergoes the biaxial tensile stress. The value of stresses depends on the friction co-efficient between punch and blank up to a great extent.
- **Wall Region:** This region is subjected to the circumferential and longitudinal tensile stresses.
- **Flange Region:** The metal from the flange region is being drawn towards the centre because of that compressive hoop stress is induced in flange. Radial compressive stress is induced due to the blank holding force. It is also subjected to the radial tensile stress.

### 1.3.4 Material Deformation in Deep Drawing

The mode of deformation of the material in deep drawing is different in the different regions due to the variable state of stresses in the respective regions. Based on this we can classify it into the following regions.

**The Flange zone:** As explained in the previous section that this region is subjected to the tri-axial state of stress, compressive & tensile radial stress and compressive hoop stress. Maximum of the deformation occurs in the flange area. Punch draw the metal and forces it into the die, due to this flange thicken at some place. As a result of flange thickening at the some places the contact between the binder and the sheet is not uniform as it was in the start of the process [4].

**The Die Radius Zone:** In this zone the metal bends & unbends over the die corner radius. The state of stress in this zone is that of radial elongation and bending over the die radius. If the die corner radius is too small, the fracture may appear in this zone. If it is having too great value, then it decreases, the draw depth and the formability of the metal is not wholly utilized. Hence, the die corner radius should be selected properly according to the set guidelines.

**The Wall Region:** The state of stress in this zone is that of radial and circumferential tension. If the punch die clearance is large, the unsupported regions of the cup wall may experience a form of undergo out-of-plane deformation (similar to wrinkling) called puckering. The punch force is transmitted from the bottom of the cup to the deformation zone (flange) through tension on the wall of the cup. The tension must not cause the wall to deform plastically; otherwise, fracture may occur [1,4].

**The Punch Radius Region:** In this zone, the sheet material undergoes bending over the punch corner radius and the state of stress is again that of radial tension. As the material bends over the die radius, it undergoes strain hardening. Hence, the flowing material, which forms the cup wall, becomes strengthened. The material at the punch corner radius is the most common failure site: the cup wall is weakest here because the portion of the sheet in this region has the least strain hardening.

**The Bottom Region:** In this region, because of greater friction between the punch surface and the bottom of the cup, the material does not undergo much plastic deformation.

### **1.3.5 Formability of the Sheets**

Formability is ease with which a sheet metal component is formed or drawn in the desired shape without undergoing localized necking or fracture. Sheet metal processes such as deep drawing, bending etc require large tensile deformation. Therefore, the problems of localized deformation called necking and fracture due to thinning down are common in many sheet forming operations. Anisotropy also is a major concern in sheet metal operations. When a sheet metal is subjected to plane strain deformation, the critical strain, namely, the strain at which localized necking or plastic instability occurs can be proved to be equal to  $2^n$ , where  $n$  is the strain hardening exponent. For uniaxial tensile loading of a circular rod, the critical or necking strain is given to be equal to  $n$ . Therefore, if the values of  $n$  are larger, the necking strain is larger, indicating that necking is delayed. In some materials diffuse necking could also happen. Simple uniaxial tensile test is of limited use when we deal with formability of sheet metals. This is due to the biaxial or triaxial nature of stress acting on the sheet metal during forming operations. Therefore, specific formability tests have been developed, appropriate for sheet metals.

#### **1.3.5.1 Formability Tests**

Some of the widely used formability tests have been described below:

##### **1.3.5.1.1 Erichsen Test**

The test consists of stretching a sheet specimen by means of a hemispherical punch until the occurrence of fracture. The depth of the punch indentation in the specimen expressed in millimeters is the Erichsen index (IE). This is the most commonly used parameter for expressing the formability of sheet metals.

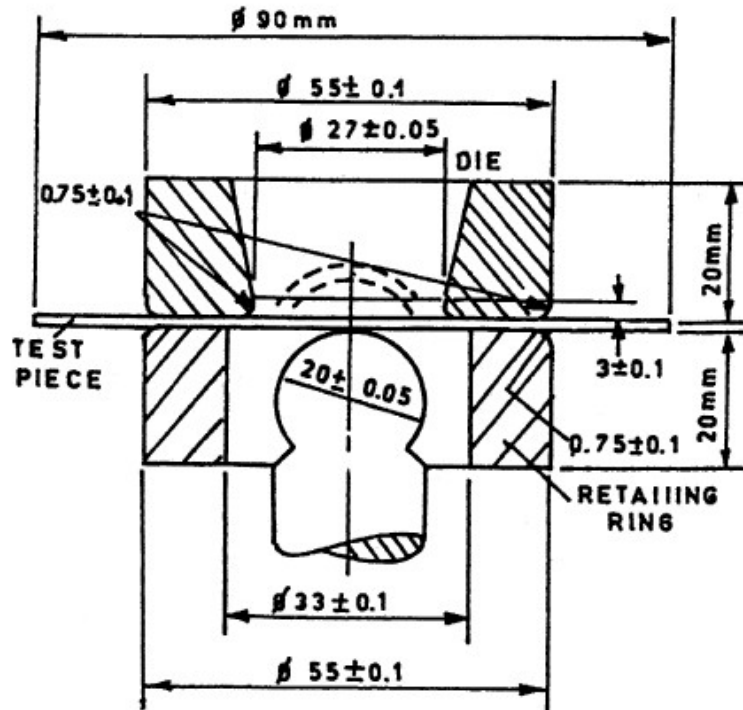


Fig.1.7 Erichsen Test [31]

### 1.3.5.1.2 Swift's Cup Test

This test consists of deep-drawing cylindrical parts having different diameters and determining the limit drawing ratio LDR. Swift's method has been widely used and is considered as a standard test by the International Deep-Drawing Research Group (IDDRG). [32, 33]

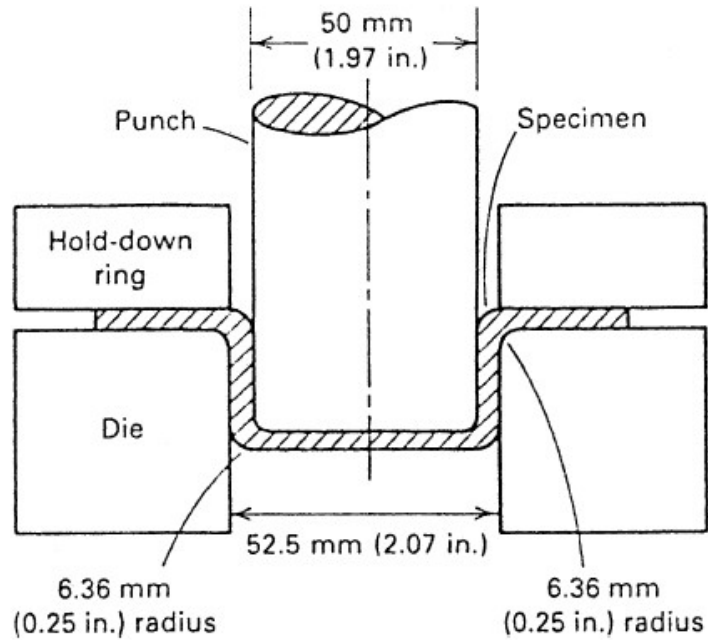


Fig. 1.8 Swift's Cup Test [34]

### 1.3.5.1.3 Fukui Test

Fukui proposed a deep drawing test using a conical die. The advantage of this method is that the 'diameter ratio'  $D/D_0$  ( $D$  = upper diameter of the part at fracture) as a measure of formability may be established by a single test.

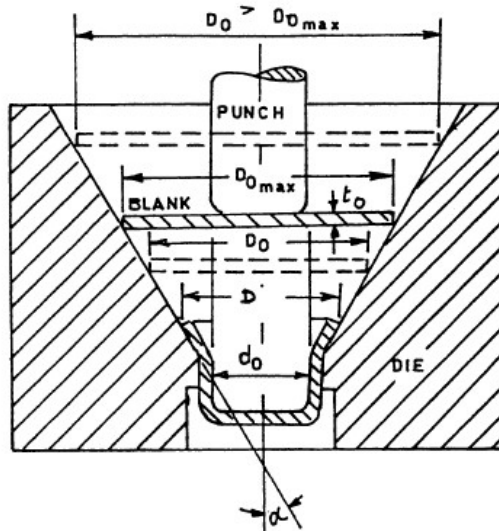


Fig. 1.9 Fukui Test [35]

### 1.3.5.2 Forming Limit Diagram

The forming limit diagram, *FLD*, is a study tool, for forming operations, that indicates how close the material is to failure, i.e. necking or fracture. The forming limit curve, *FLC*, defines the maximum strain combinations that a metallic sheet can undergo for different forming conditions, such as deep drawing, stretching, bending and die drawing, without failure. The FLC can be empirically constructed by using a hemispherical punch biaxial stretch test, as well as a tension test to strain the specimen and then recording the major and minor strains,  $\epsilon_1$  and  $\epsilon_2$  just before necking or before fracture occurs. Note, however, that in practice there are scatter in the measured strains, just prior to failure, and therefore one do not consider a single curve but rather a band in which necking or fracture is likely to occur.

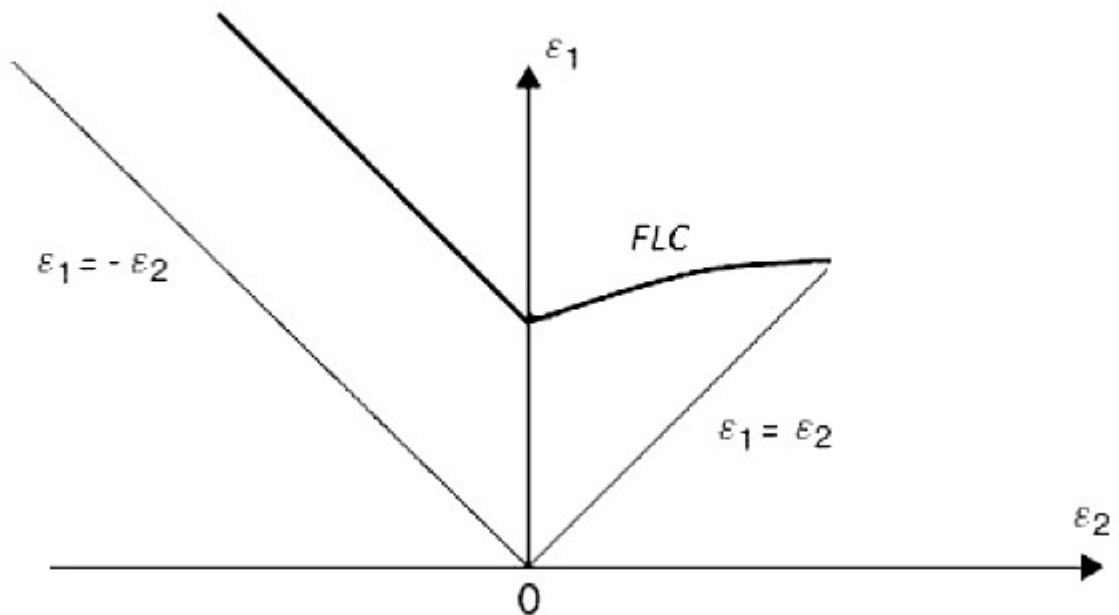


Fig. 1.10 Forming limit curve showing different strain combinations responsible for failure. [36]

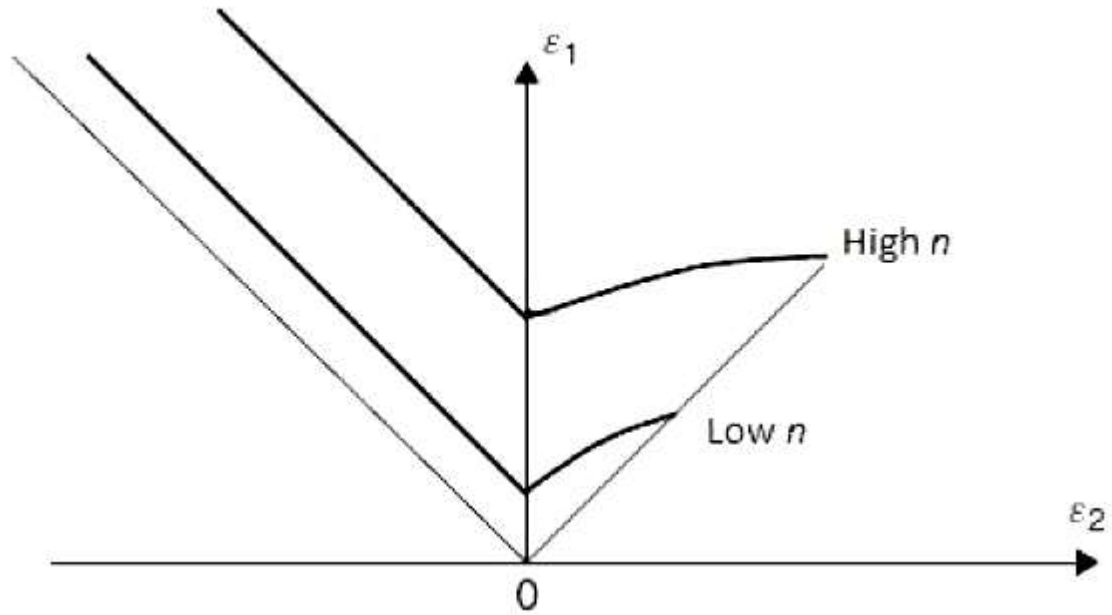


Fig. 1.11 FLC for the low and high values of work-hardening co-efficient. [36]

### 1.3.6 Limiting Drawing Ratio

Drawability can be defined as the capability of the blank to be drawn effectively from the flange into die cavity using a punch with a particular radius. The magnitude of the deformation of a deep drawn part is usually characterized by a drawing ratio  $\beta$ , which is defined as the ratio of the initial blank diameter  $D_0$  to the inside diameter of the finished cup  $D_p$ . The larger the chosen drawing ratio, the larger will be the drawing load under otherwise constant conditions. This load must be transmitted by the wall of the deep drawn part. Therefore, the drawing ratio must not exceed a maximum value, limiting drawing ratio in order to prevent cracks at the bottom of the cup. This Limiting Drawing Ratio is defined as the ratio of the maximum diameter of the circular blank to the diameter of the used punch, which can be attained without failure.

$$\text{LDR} = (D_0/D_p)_{\max} = e^{\eta}$$

where  $\eta$  is the efficiency of drawing.



The maximum LDR for efficiency =100% is equal to 2.7.

If we assume an efficiency of 70% the maximum LDR is about 2. That means the maximum reduction possible in single deep drawing step is 50%. This is the general criteria for first draws.

### 1.3.6.1 Redrawing

Redrawing is reduction in diameter and increase in length of a cup which has been drawn to a certain draw ratio. In case of materials which are difficult to draw in one step, redrawing is performed. Generally, during the first stage up to 40% reduction is achieved. In the first redrawing after drawing, maximum of 30% reduction can be set. In the second redrawing stage, 16% reduction is set. In direct redrawing process, the angle of bending undergone by the cup is less than  $90^\circ$ , thereby reducing the draw force.

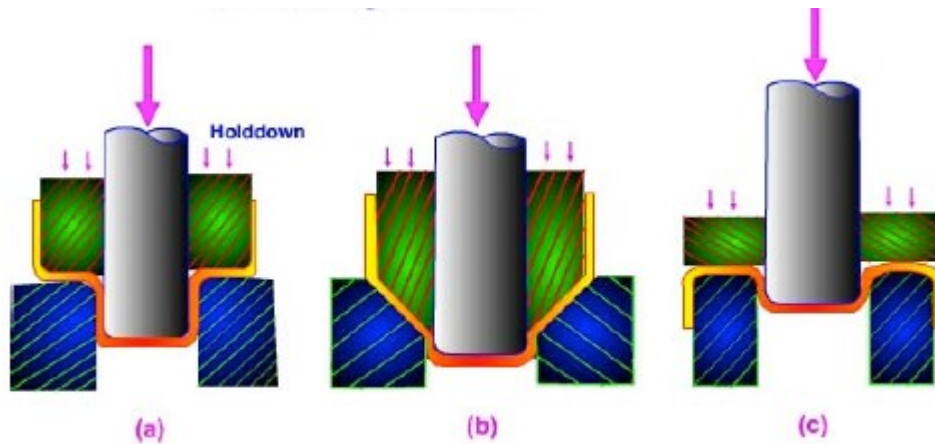


Fig. 1.12 Redrawing methods (a) Direct redrawing (b) Direct redrawing with taper die (c) Reverse redrawing

### 1.3.7 Factors Affecting Deformation Deep Drawing

In this following section various factors controlling the deep drawing operation are analyzed. However, it must be noted out that a hierarchy exists among the different factors, these factors can be divided into three categories: geometric, physical & material parameters.

### **1.3.7.1 Design Parameters**

The design of the die and punch affects the metal flow & friction conditions in the deep drawing process. The influence of the different parameters is discussed in following section.

#### **1.3.7.1.1 Die Corner Radius**

The die corner radius ( $r_d$ ) depends on the thickness and size of the blank. Theoretically, larger die corner radius reduces the draw load and increases the limiting draw ratio. However, if the draw corner radius is too large, it reduces the contact area between the flange and the blank holder and increases the tendency to wrinkle. Too sharp die corner radius will hinder the normal flow of the metal and cause uneven thinning of the cup wall, resulting in tearing. Smaller die corner radii may cause confined failures in the bending zone by increasing the strain hardening tendency. If the die corner radius is small, the interaction with the tools is also less which may cause a heat upsurge, leading to the deteriorating of the die material and more rapid erosion. It was also concluded that too much increase of the die corner radius does not significantly increase the limiting draw ratio and may lead to wrinkling or puckering. So a safe region of  $2t \leq r_d \leq 10t$  is desirable in most of the sheet metal forming operations. The die corner radius may be increased to 6 to 8 times the metal thickness when drawing shallow cups on heavy gauge metals without blank holder. [1,2]

#### **1.3.7.1.2 Punch Corner Radius**

In sheet metal forming punch corner radius is very crucial since most of the time fracture occurs nearer to punch corner radius. A sharper radius will require higher forces where the metal is folded around the punch corner and results in excessive thinning or tearing at the bottom of the cup. To prevent excessive thinning, the punch corner radius ( $r_p$ ) must be within the range of 4 to 10 times the metal thickness ( $t$ ). If the radius of punch is less than four times the blank thickness, it may be necessary to form it over a larger punch radius and then re-strike it to develop the specific radius.

The radius may be determined by the product design when only one draw is necessary to complete the work piece because the cup bottom takes the shape of the punch corner. The empirical findings of the experiments show that for  $r_p \leq 2t$ , the cup is more prone to the tearing failure while for  $r_p \geq 10t$ , stretching may be pronounced. Further, it is also observed that within the range of  $4t \leq r_p \leq 8t$ , punch corner radius does not significantly affect limiting draw ratio. (The smaller the punch corner radius, the greater amount of such formations and re-formations the metal has to go through. If too much, such process results in larger spring back). [1,3]

#### **1.3.7.1.3 Radial Clearance**

Radial clearance is very crucial parameter in deep drawing operations. It is the difference between die radius and punch radius ( $w_c = DR - PR$ ). The clearance between the punch and die throat affects the flow region and geometry of the cup. The optimum value of the clearance can be fixed by two factors: blank thickness & material type. For thinner blanks, the clearance should be as tight as possible to prevent worn out edges. However, for thicker blanks the value of clearance should be higher to allow the perforating process to be successful without having harmful effects on the punch and the die and to give a good edge quality. As the blank is strained over the die radius, there is steady decrease and then increase in the thickness of the blank. The value of draw force increases as the clearance decreases. A secondary peak occurs on the force-stroke curve where the blank thickness is slightly greater than the clearance and where ironing starts. When clearance is equal to the blank thickness, ironing of the metal will occur near the top of the cup. It is revealed that the distribution in sheet metal thickness is increasing with dipping value of the radial clearance ( $w_c$ ). In addition, for the radial clearance ( $w_c$ ) that is less than the blank thickness ( $t$ ), the cup fails due to increased thinning. Whilst for the radial clearance ( $w_c$ ) greater than the blank thickness ( $t$ ), thinning is stable. The radial clearance which is less than  $(0.5t)$  is not suitable because the fraction of decrease in thickness is more than 45%, while the utmost acceptable percentage of reduction in thickness is 45% [1]. It is made known that the spring back fraction is reduced with

increasing the radial clearance (wc). As well, for the radial clearance (wc) that is less than the blank thickness (t), the cup fails due to increased thinning.

#### **1.3.7.1.4 Blank Thickness**

The original blank thickness has some outcome on the thickness distribution and thinning of blank in the deep drawing operations. The average distribution of the blank thickness is increasing with increasing the blank thickness. Also, the fraction of thinning is increasing with increasing the blank thickness. Slightly thicker blanks can be gripped better during the deep drawing operations. Also, thicker blanks have more volume and hence can be long-drawn-out to a greater extent with increasing in thinning. The original blank thickness has some effect on the spring back of sheet metal in the deep drawing operations. It has been revealed that the spring back fraction decreases with increasing the blank thickness [1].

#### **1.3.7.2 Material Parameters**

Flow stress, strain hardening co-efficient, anisotropy and microstructure are the important material variables in the analysis of the sheet metal forming for a given composition and deformation. Both flow stress and anisotropy influence the forming behavior. Further, they also affect the deformation behavior of the metal. Stretch ability of metal is significantly affected by strain-hardening exponent (n) governing the neck strain distribution.

##### **1.3.5.2.1 Anisotropy**

An plastic anisotropy,  $\bar{r}$ , is calculated as:

$$\bar{r} = \frac{r_0 + 2 r_{45} + r_{90}}{4}$$

Where  $r_0, r_{45}$  and  $r_{90}$  are r-values at  $0^\circ, 45^\circ$  and  $90^\circ$  from the rolling direction.

Increasing r-values decrease the force required to deform the flange while increasing the strength of the cup wall. The r-value indicates the ability of the material to resist

thinning. When  $r > 1$ , the material flows easily in the plane of the sheet but not in the thickness direction. On the other hand,  $r < 1$  means that the material flows easily in the thickness direction, and this is an undesirable property as it might lead to excessive thinning.

For an anisotropic material, drawability will be given by

$$\ln(\text{LDR}) = \sqrt{(r + 1)/2}$$

Planar anisotropy,  $\Delta r$ , is calculated as:

$$\Delta r = \frac{r_0 - 2r_{45} + r_{90}}{2}$$

The higher the values of  $\Delta r$ , the more earing occurs. Earing typically must be trimmed; therefore, an increase in  $\Delta r$  increases trimming and reduces the total depth of draw.

#### **1.3.7.2.2 Strength Co-efficient**

A high **K**-value means a strong wall, which is beneficial, but also a strong flange, which makes it harder to draw in. Therefore, for the drawing operation to be successful, the **K**-value should be sufficiently large to assure a product of reasonable strength, but not so high such that it necessitates use of large punch force to complete the draw, which in turn might cause fractures.

#### **1.3.7.2.3 Work Hardening Co-efficient**

The work hardening coefficient ( $n$ ) and the anisotropy value affect the magnitude of the limiting draw ratio. Sheet metal with good deep drawing characteristics should have a high  $r$ -value and small planar anisotropy. Sheet metal for combined forming by deep drawing and stretch forming should both have a high normal anisotropy value and a high work hardening coefficient. The bottom tearing force in deep drawn cups is also affected by the work hardening coefficient: A larger

value of work hardening results in an increase in transferable load on deep drawn work-piece; a higher work hardening coefficient also means higher strain before necking. Depending on the type of forming process (deep drawing or stretch forming), the normal anisotropy (  $r$  ) work hardening coefficient (  $n$  ) will have a decisive role in determining the material behavior. Thus the limiting draw ratio increases with, increasing  $r$ -value and produces less thinning in transition region from cup bottom to the wall and also reduces the drawing load. [36]

### 1.3.7.3 Process Parameters

#### 1.3.7.3.1 Blank Holding Force

The blank holding force (BHF) necessary to hold a blank flat for a cylindrical draw varies from very modest to utmost of one third of the drawing force. The higher the value of binder force, the larger will be the strain over the punch face, however the process is restricted by the strain in the side-wall. If the tension is reached to its maximum value, the side-wall will fail by splitting. It has been shown that the spring back percentage is stable with increasing of blank holding force (BHF) up to a certain value. After that the spring back percentage is increasing with increasing of BHF [4]. Comparison between the draw depth and blank holding force is shown in figure 1.13.

$$p_{BH} = 10^{-3} c \left[ (DR - 1)^3 + \frac{0.005d_0}{t} \right] \sigma_{uts}$$

$$F_{BH} = p_{BH} \times A_{BH}$$

$p_{BH}$  is the blank holder pressure

$F_{BH}$  is the blank holding force

$A_{BH}$  is the area of the blank holder

$c$  is the empirical factor, ranging from 2 to 3

$DR$  is the drawing ratio

$d_0$  is the blank diameter

$t$  is the blank thickness

$\sigma_{uts}$  is the ultimate tensile strength of the sheet material

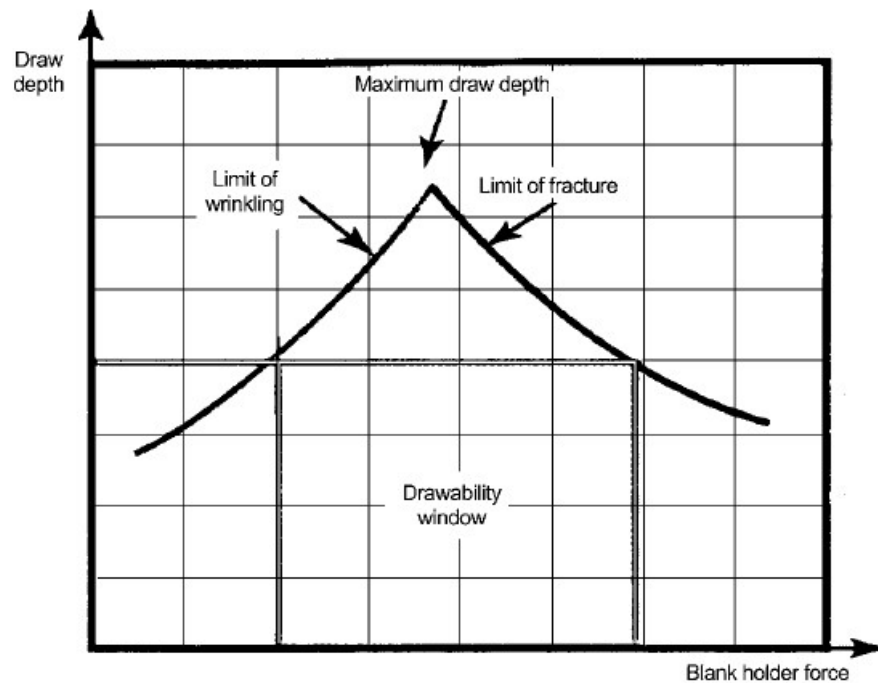


Fig. 1.13 Graph showing variation of draw depth w.r.t blank holding force. [30]

### 1.3.7.3.2 Friction

In Sheet Metal Forming operations, such as deep drawing, friction plays a significant role. Together with the deformation of the sheet, the friction determines the essential punch force and the binder force. As a result, the friction influences the energy which is desirable to deform a blank. Friction also influences the stresses and strains in the blank and, hence, the quality of the drawn product.

#### **1.3.7.3.2.1 Co-efficient of friction between punch & blank**

The drawing force that is necessary to form the blank is applied by the punch on the bottom of the cup and transferred from there to all the way through the wall into the flange. This transmission of force calls for the highest possible coefficient of friction on the punch edge. This demonstrates the first important rule for lubrication in this case: neither the punch nor the blank should be lubricated in this area. Even if this consideration is optimal for an isolated forming operation and force transfer, one still must consider punch wear. For fluid lubricant, it has been revealed that the distribution in blank thickness is decreasing with increase in value of the coefficient of friction between punch and blank. For solid lubricant and dry lubricant, the distribution in blank thickness is steady with increasing the coefficient of friction between punch and blank [1,2].

#### **1.3.7.3.2.2 Friction Co-efficient between blank and holder**

The primary motive of deep drawing lubrication is to attain minimum friction in the binder area. This includes the lubrication on the binder side, which, as much as possible, should be a lubricant ring in order to reduce the friction in the region of the punch edge to make it as little as possible. However, in the case of high viscosity oils and drawing pastes, if the applied lubricant film is excessive, there is the risk that hydrostatic effects on the blank holder side of the flange can cause reduction of sheet metal contact with the blank holder resulting in wrinkling. When the coefficient of friction between binder and blank increases, the spring back percentage is decreasing. [1]

#### **1.3.7.3.2.3 Friction Co-efficient between Die and Blank**

The major aim of the lubrication in the die and blank interface region is to trim down wear. Thinning fraction increases with increase in value of co-efficient of friction between die and blank. On the other hand the spring back effect decreases with increasing value of friction co-efficient.



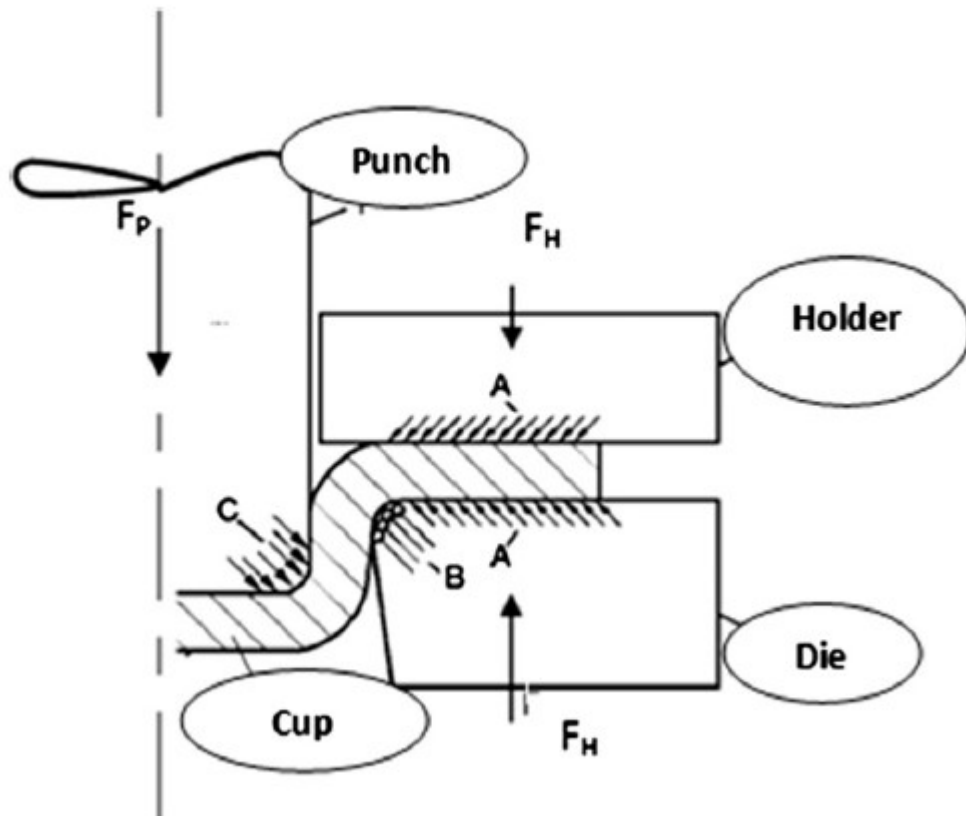


Fig.1.14 Friction regions in a deep drawing a cup. (A) Friction surface between blank and binder & die; (B) friction surface between blank & the die corner radius and (C) friction surface between blank & the punch corner radius;  $F_p$ , total drawing force;  $F_H$ , blank holding force.[1]

### 1.3.7.3.3 Punch Velocity

The punch penetrates the blank at a certain velocity which has specific effect on the success of drawing operation. Slower drawing speeds must be used for lesser ductile metals. When too much thinning occurs, the drawing speed must be reduced. The idyllic conditions that have to be maintained to obtain most favorable drawing speeds are the adequate lubrication, cautiously controlled binder pressure and the condition of the press which are to be maintained at high level of accuracy. The punch velocity in hydraulic press is fairly constant throughout the stroke. In mechanical presses, punch velocity is taken as that at mid-stroke because the velocity changes in a characteristic manner throughout the

drawing stroke from maximum velocity to zero. The drawing speed has greater influence in drawing stainless steel and heat resistant alloys than in drawing softer and ductile metals. Higher press speeds may cause cracking and excessive wall thinning while drawing metals with lower ductility.

### **1.3.8 Defects in Deep Drawing**

The deep drawing process depends on the number of factors as explained in the previous section. If the specific values of these parameters not maintained then defects occurs in the drawn part. Defects set the limit of drawing or stamping in the sheet metal processes. The most common and frequent defects are like wrinkling, tearing, orange peels, earing , necking and scratching.

- **Wrinkling:** Wrinkling takes place when one of the principal stress is compressive in nature. The circumferential compressive stress cause the problem of wrinkling or buckling. The wrinkling can be avoided by using the appropriate value of the blank holding force. Wrinkling takes place on the both flange as well as on side walls.
- **Earing:** When the walls of the drawn part or cup have peaks and valleys this defect is known as earing. Planar anisotropy is the only cause behind the wave edges on the drawn part. There might be two, four and six ears but four numbers of ears are very common.

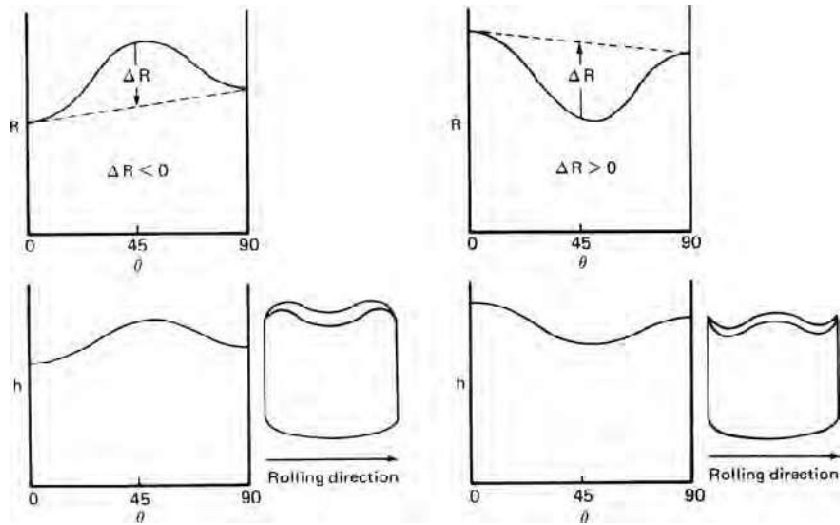


Fig. 1.15 Earing defect w.r.t rolling direction

- **Tearing or Localized Necking:** In the starting of a tensile deformation the process is stable and homogenous over the work-piece. However, at some stage, large amounts of strain might localize in a small region and the local cross-sectional area will decrease. This is called a neck in the material. If the deformation continues, almost all deformation will be concentrated in the neck and this instable deformation will eventually lead to tearing of the material. The reason for necking is due to the fact that all real materials are imperfect, in the sense that they have small local variations in dimensions and composition, which lead to local fluctuations in stresses and strains.
- Besides these defects there are several types of surface defects like Luder lines, orange peel effect, ring prints etc. Orange peel effect defect is mostly cause by the increase in the grain size of the part during the drawing process. Luder lines or stretcher strain is a commonly found defects in the low carbon steel drawn parts. Its appears like a flame type pattern of the impression on the surface.

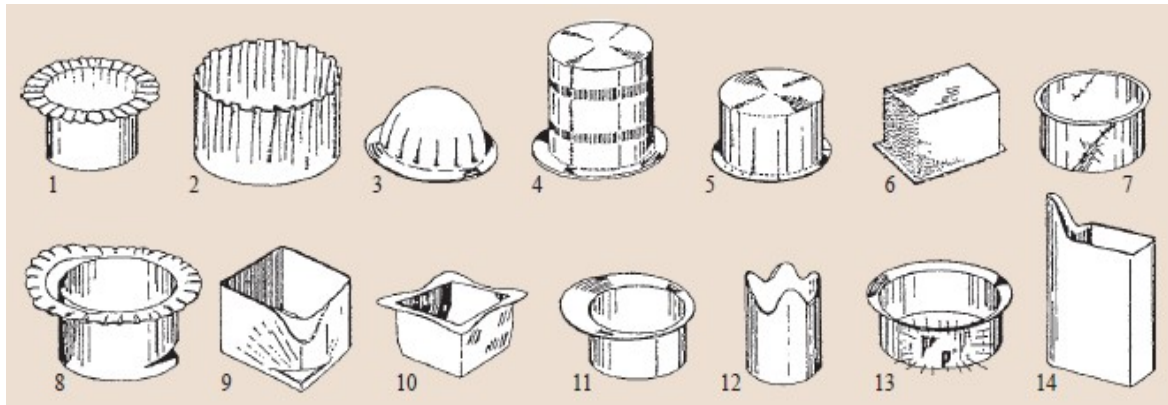


Fig. 1.16 Various failure modes in deep-drawing: 1-flange wrinkling; 2-wall wrinkling; 3- part wrinkling; 4-ring prints; 5- traces; 6-orange skin; 7-Lüder's lines; 8-bottom fracture; 9- corner fracture; 10,12-folding; 13,14-corner folding. [29]

## 1.4 Motivation

## 1.5 Objective

The major objectives of this project can be identified in the following list:

- Selection of materials for fuel tank and determining their tensile properties.
- To design the die face of fuel tank using the die module in the HYPERFORM<sup>®</sup>.
- Creating a tool and die setup in the Incremental RADIOSS with suitable die clearance and binder surface.
- Analyzing the results of the simulation and propose the appropriate changes in the forming parameters to avoid draw defects like wrinkling, thinning and cracks.
- Simulating the process using different material under the varying thickness and analyzing their effects on the deep drawing process.
- Prediction of FLD using HYPERFORM<sup>®</sup>.

## **1.6 Organization of Thesis**

The chapters of the thesis are arranged in the following manner. *Chapter one* presents the background of this project along with the objectives. Besides that it describes the deep drawing process and its various parameters and their effects on the process. *Chapter two* provides a inclusive literature review related to various aspects of the deep drawing process. *Chapter three* deals with the die face design and generations of tool and binder using the die face in Incremental RADIOSS. *Chapter four* the material properties and stress strain diagram are defined in this chapter. *Chapter five* provides the results obtained by the simulation study. Finally, *Chapter six* concludes the thesis and provides suggestions for future work.

## CHAPTER 2

### LITERATURE REVIEW

With an aim to review the different technical concepts that are utilized in the deep drawing process as well as to disclose the influence of the key process parameters on the excellence of drawn products, a literature review is presented in this chapter.

M. El Sherbiny [1] used the parametric analysis technique that is utilized in ABAQUS modeling software for creating the three dimensional numerical simulation for the sheet drawing process. ABAQUS runs on the FEA program and it is supplied with the material properties and boundary conditions as an input data. With the developed simulation model, one can easily determine the thickness distribution, thinning and the maximum residual stresses on the blank side at the various die design parameters. To validate the simulation model, he compared the data obtained from simulation with the experimental results of Colgan and Monaghan. This comparison results into the agreement of the two methods, that is simulation and experimental. The simulation used definitely reduced the time and cost of analyzing the deep drawing process on different parameters.

Hill. R. [6] analysed the pure radial drawing of an annular flange assuming a rigid plastic material. Plane strain and plane state of stress conditions were considered. An isotropic material was chosen and it is assumed that there is negligible frictional force in the process. Levy Mises rule and the Tresca theory were assumed together. He made the conclusion that the generalized strain and the circumferential strain occurring in the flange portion are equal in magnitude. He showed the location of the particles in the deforming flange and proved that there was little dependence on the stress-strain properties of the material. There was greater tendency of work hardening and reduction of thickness of material across the annulus at any moment.

Chung S.Y. and Swift H.W. [7,8] extended the work to consider the friction at the rim of the blank. Their assumptions were justified by detailed comparison with their experimental work. Swift's work led to a good understanding of radial drawing and to an appreciation of thinning of material as it passes over the die. They reported punch load for different travel positions of punch. Chung and Swift pointed out that their theory is not capable of predicting strains over the punch head, where critical conditions generally occur leading to fracture. Their theory can be used for predicting punch loads and power requirements, however, although the computation is necessarily complicated and is not recommended for general use.

Lankford W.T. et al [9] recognized the importance of the variation of r-value with orientation in the plane of sheet for commercial low carbon steel. They reported that the variation in r-values could be exploited for unsymmetrical stampings. The variation of the plastic behavior with direction is assessed by a quantity called Lankford parameter or anisotropy coefficient which is determined by uniaxial tensile tests on sheet specimens in the form of a strip. The anisotropy coefficient ( $r$ ) is defined by

$$r = \frac{\epsilon_2}{\epsilon_3} \quad (2.1)$$

where  $\epsilon_2$  ;  $\epsilon_3$  are the strains in the width and thickness directions, respectively.

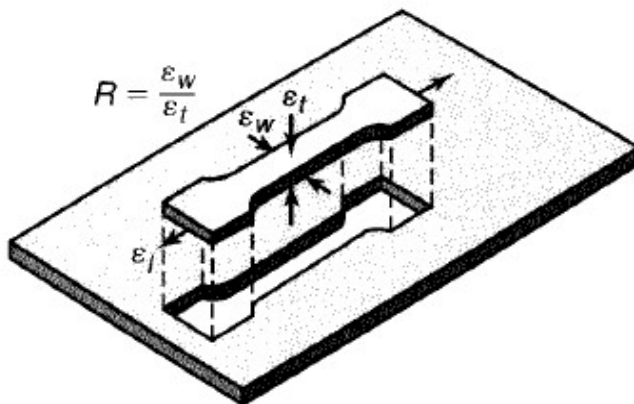


Fig.2.1: Strains on a tensile-test specimen removed from a piece of sheet metal.

Equation 2.1 can also be written as

$$r = \frac{\ln \frac{b}{b_0}}{\ln \frac{t}{t_0}} \quad (2.2)$$

where  $b_0$  and  $b$  are the initial and final width, while  $t_0$  and  $t$  are the initial and final thickness of the specimen, respectively.

Taking into account the condition of volume constancy,  $\epsilon_1 + \epsilon_2 + \epsilon_3 = 0$ , following form of 2.1 is obtained

$$r = - \frac{\epsilon_1}{\epsilon_2 + \epsilon_1} \quad (2.3)$$

and 2.2 becomes

$$r = \frac{-\ln \frac{b}{b_0}}{\ln \frac{t}{t_0} + \ln \frac{b}{b_0}} \quad (2.4)$$

El-Sebaie M.G. et al [10] presented theoretical results of  $n$  and  $r$  on the limiting draw ratio when drawing with a flat headed punch. They concluded through experiments that  $n$ -value has little effect on limiting draw ratio and while increasing  $r$ -value increases the draw ratio. They have shown that at least two instability modes are possible. The first mode in the cup wall occurs under plane strain tension and is most likely to apply to annealed materials. The second mode is in the flange under uniaxial tension and this is most likely to apply to materials that have been previously cold-worked. The limiting drawing ratios for drawing with rough punch are somewhat greater than those for drawing with smooth punch.



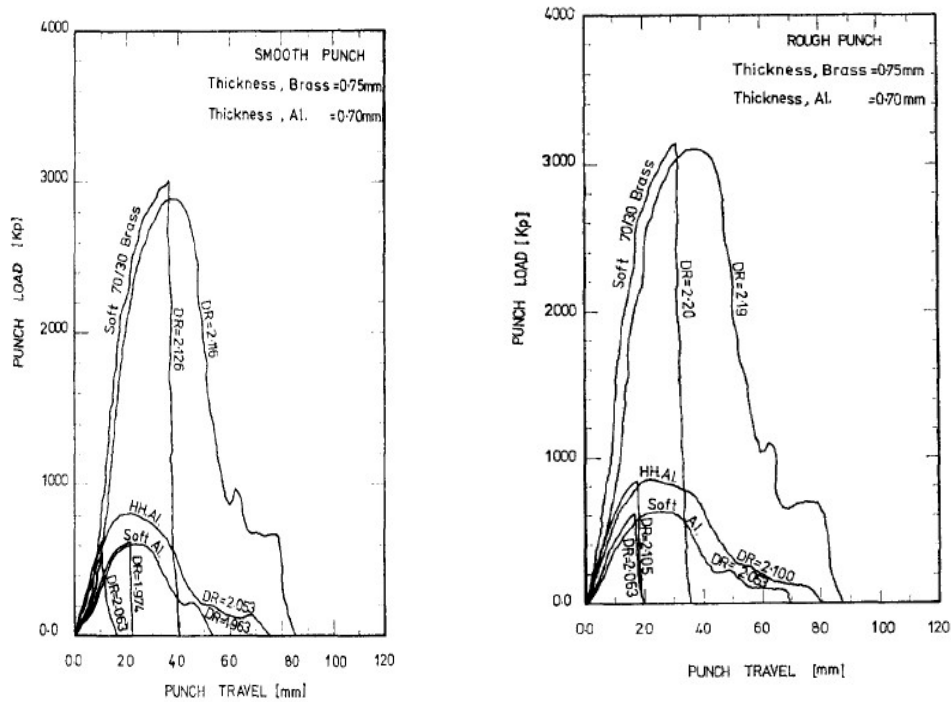


Fig.2.2: Punch load/travel diagrams for all materials drawn with (a) smooth punch (b) rough punch

Darendeliler H. et al [11] developed finite element method to study elasto-plastic deformation of sheet materials in the presence of large strain and displacements. They have assumed the sheet material to be isotropic and insensitive which obeys  $J_2$  flow theory. The work hardening characteristics of the material and Coulomb friction between sheet metal and punch were considered with a constant blank holding force.

Yang D.Y. and Lee H.S. [12] suggested that deformation region can be divided into several zones by considering geometric characteristics and contact boundary conditions. An elliptical punch was used and experimental results were compared with computed results and found to be in good agreement with experimental value for the punch load and thickness strain distributions.

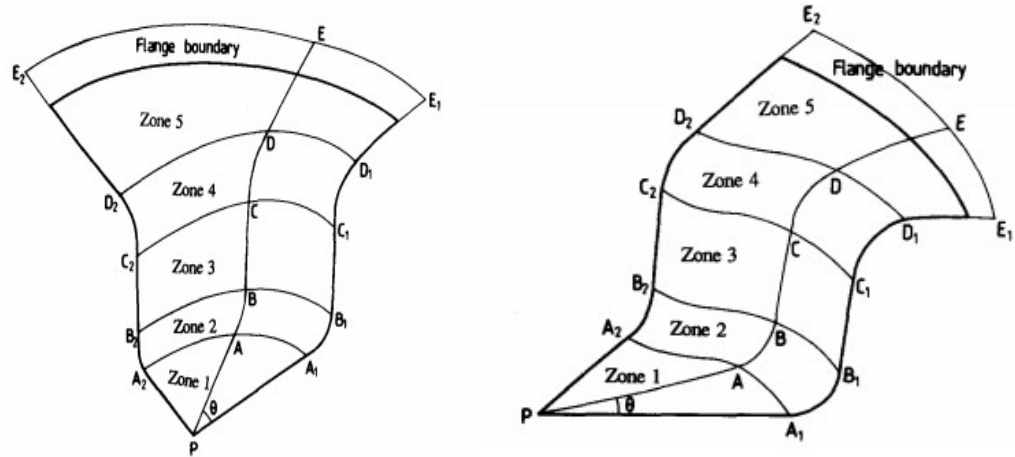


Fig.2.3: (a) Schematic diagram of five regions in the deep drawing by an elliptical punch. (b) Schematic diagram of five regions in the deep drawing by a clover-type punch.

Lee C.H. and Kobayashi. S [13] described the matrix method for the analysis of rigid-plastic deformation problems and demonstrated its use to analyse simple compression of cylinders and plane stress hole expansion and flange drawing of planar anisotropic sheets. The matrix method enabled the computation of free surface barreling and produced the so-called "folding" that has been a long known fact but never shown by a theoretical calculation previously.

Michal J. Saran et al [14] developed a formulation for numerical simulation of complex forming with special emphasis on accuracy and computational efficiency. An incremental displacement approach based on Lagrangian formulation with elastic visco-plastic material model with Hill's cross-anisotropy, power law hardening and strain rate sensitivity are assumed was attempted. Adaptive remeshing procedures were adopted which reduced the number of elements while maintaining the same level of accuracy. They concluded that strain distribution agrees with the experimental values.

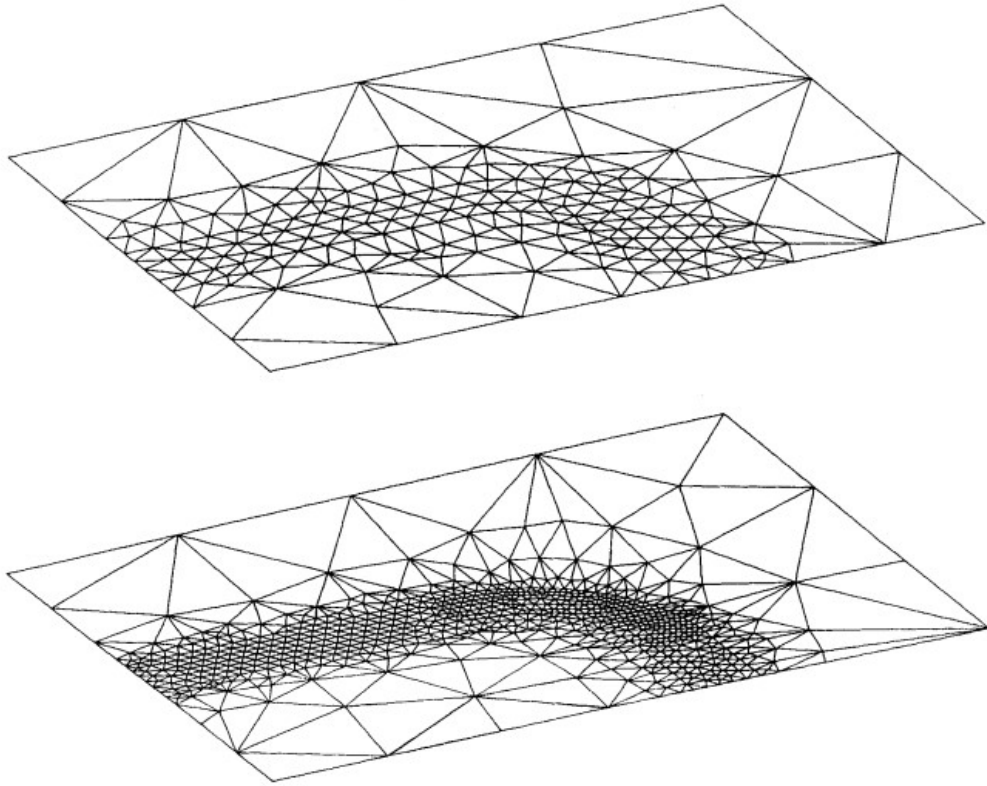


Fig.2.4: Adaptively redesigned meshes for the test part example

Seo [15] investigated the work hardening of the material during multiple forming. The thrust of his work was on the loss of ductility due to cumulative work hardening during multiple deep drawing. A three-dimensional model was used to conceptualize the design necessary to set up finite element models. The results of his work showed that work hardening induced from the first draw station affects material deformation behaviour in subsequent forming. The aim of the investigation was to predict material fracture upon reaching a final shaping station.

Jain et al. [16] conducted simulations on the progressive-die-sequence design for automotive parts. The objectives of their investigation were to determine the number of forming stages, tool geometry for each stage, drawing depth in each forming stage and the blank holder force for each stage. They concluded that the integration of simulations and past experience can reduce the number of die tryout tests and associated time and cost. Furthermore, they concluded that integrating simulations

allows further refinement and optimization of the die design to improve product properties such as wall thickness tolerances.

Keeler[17] pioneered the research in the field of Forming Limit Diagrams (FLDs). He demonstrated that the maximum values of the principal strains  $\epsilon_1$  and  $\epsilon_2$  can be determined by measuring the strains at fracture on sheet components covered with grids of circles. During forming the initial circles of the grid become ellipses. Keeler plotted the maximum principal strain against the minimum principal strain obtained from such ellipses at fracture of parts after biaxial stretching ( $\epsilon_1 > 0$ ;  $\epsilon_2 > 0$ ) [18]. This way he obtained a curve limiting the tolerable range.

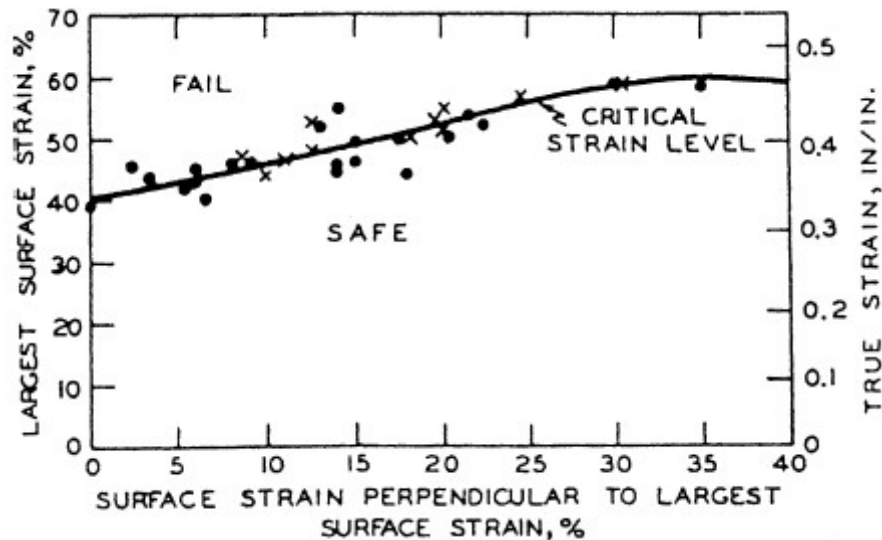


Fig.2.5: Forming limit diagram defined by Keeler [17]

Goodwin [19] plotted the curve for the tension/compression domain ( $\epsilon_1 > 0$ ;  $\epsilon_2 < 0$ ) by using different mechanical tests. In this case, transverse compression allows for obtaining high values of tensile strains like in rolling or drawing.

The diagrams of Keeler (right side) and Goodwin (left side) are currently called the Forming Limit Diagram (FLD), see Fig. . Connecting all of the points corresponding to limit strains leads to a Forming Limit Curve (FLC). The FLC splits the ‘fail’ (i.e. above the FLC) and ‘save’ (i.e. below the FLC) regions. The Forming Limit Curve (FLC) is plotted on a Forming Limit Diagram (FLD). The intersection of the limit

curve with the vertical axis (which represents the plane strain deformation ( $\epsilon_2 = 0$ )) is an important point of the FLD and is noted  $FLD_0$ .

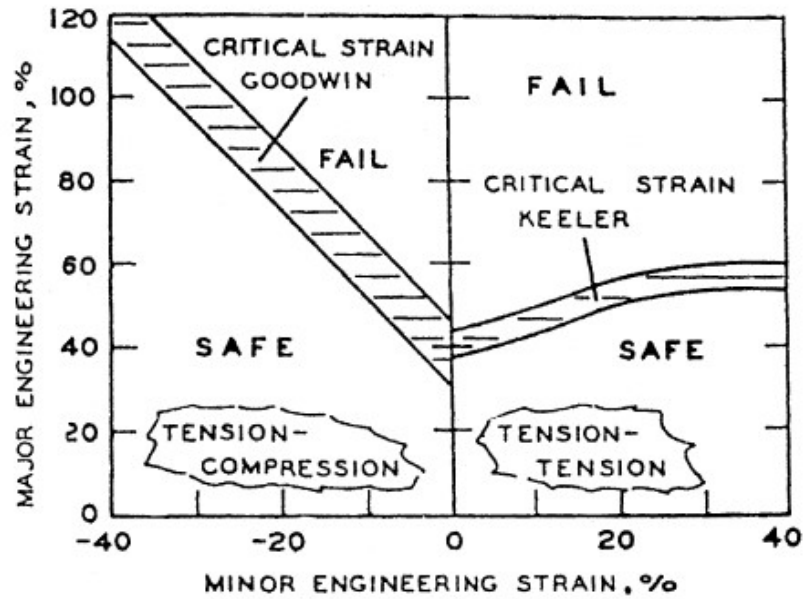


Fig.2.6: Forming limit diagrams defined by Keeler and Goodwin [19]

Today, depending on the kind of limit strains that is measured different types of FLD's are determined: for necking and for fracture, see Fig. 2.7

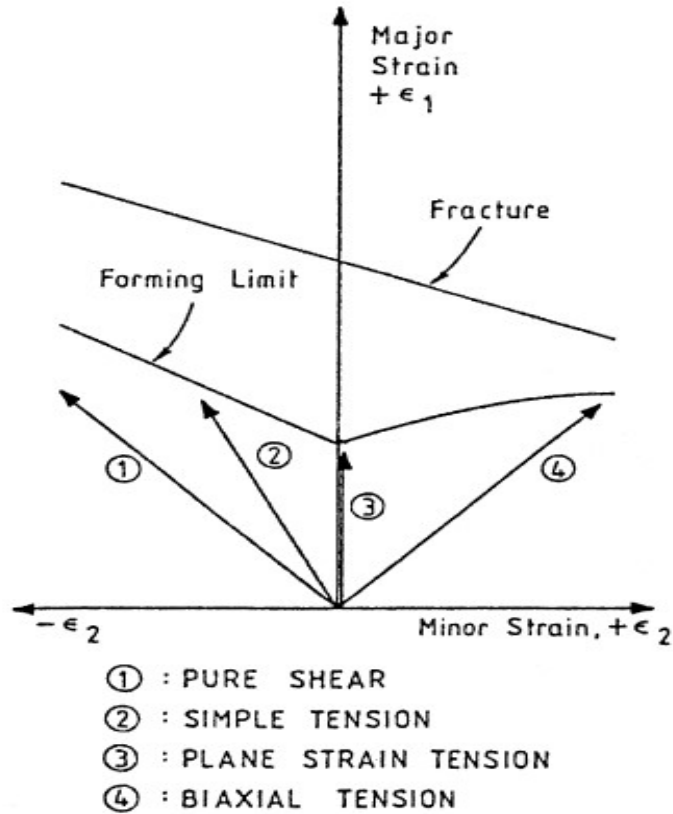


Fig.2.7: Forming limit diagrams for necking and for fracture

Kaftanoglu [20] developed a method to model flange wrinkling in axisymmetrical deep drawing using the energy method. In this approach, wrinkling occurs if the plastic work done for deep drawing is higher than the plastic work done for wrinkling. For this purpose, using von Mises yield criteria, a plastic analysis is done for the flange part of the blank, assuming plane stress conditions. For the calculation of work done for wrinkling, wrinkles are assumed to be a sine curve in shape. So the amplitude of the wrinkles are calculated, then using the plastic bending moment, work done for wrinkling is obtained. Using these procedures, plastic work versus reduction strain curves are obtained for both deep drawing and wrinkling. When the slope of the wrinkling curve is greater than deep drawing curve, wrinkling does not occur, since the energy required is greater than deep drawing. Considering the peaks of the wrinkles as plastic hinges, the blank-holder force needed to suppress wrinkling is found in terms of wave number. Experiments are conducted to verify the numerical results with several materials and for several initial blank diameters.

Ramaekers et al. [21], made a research on the deep drawability of a round cylindrical cup. The limiting drawing ratio is tried to be related with some process parameters like anisotropy factor, strain hardening exponent, etc... Upper and lower bound methods are used to obtain theoretical models. Using the theoretical model proposed for deep drawing, estimation for the limiting drawing ratio is tried to be achieved. Some experiments are conducted to verify the model developed. Comparing the results, it is seen that an agreement between the model for deep drawing and experiments. However, a precise prediction of the limiting drawing ratio could not be achieved. The friction coefficient is seen to be an important factor for the drawability of large size products. The study showed that decreasing friction coefficient, increases limiting drawing ratio.

Cao and Boyce [22] examined wrinkling and tearing type of failures in sheet metal forming. For prediction of wrinkling, they used a method proposed by Cao and Boyce. The criterion is based on the energy conservation and minimum work to suppress the wrinkling. Total strain energy values for a perfect plate and for buckling plate are recorded. Then the force/pressure needed to suppress the wrinkling is calculated using the energy difference and wrinkling amplitude. In prediction of tearing, existing forming limit diagrams are used in correspondence with the local strain histories near possible tearing regions. They also developed a technique named variable binder force in which blank-holding load varies in controlled manner, not a constant blank-holding load was used. A control algorithm is proposed for variable binder force technology. Two examples are used: conical cup drawing and square cup drawing. Finite element models of both cases are analyzed by commercial program ABAQUS. Comparison with the experimental results shows that the method is capable of predicting wrinkling and tearing. The control algorithm for variable binder force is tried in both cases, and 16% extra cup forming height is provided for conical cup drawing.

Makinouchi et al [23] analyzed wrinkling during deep drawing of conical cups numerically and experimentally. The experiments were conducted not only to create a reference for FEM simulation, but also to give some guidelines for a reliable benchmark test of the wrinkling prediction capability of various FEM codes. The simple component geometry enabled the easy comparison of experimental and FEM results. To make numerical results more general, two types of FEM analyses were employed: static-explicit (ITAS3D) and dynamic-explicit (ABAQUS/Explicit). The same simulation parameters used enabled the comparison of both techniques. The experiments were carried out with an anisotropic sheet with a view to investigate the shape of wrinkles on a hydraulic press because of its advantage in controlling load and ram velocity which can be adjusted according to the requirements of the deformation process.

Ferron et al [24] developed a bifurcation analysis for predicting the occurrence of wrinkling in metal sheets with isotropic elasticity and transversely anisotropic plasticity. Based on the local conditions describing sheet geometry, loading and material anisotropy, wrinkling is predicted in the form of a limit curve defining bifurcation in principal stress space, along with the wavelength and orientation of the wrinkles. The practical relevance of this approach was checked by comparison with FE predictions of wall wrinkling in the conical cup test in the Abaqus, a FE code. The simulations are made for different materials.

Rees [25] examined the formability of a zinc clad automotive CR sheet steel. This material's extended ductility allows a diffuse instability condition to define the limit of formability at the onset of necking under in-plane biaxial stressing. It is shown how this theory can admit material anisotropy, sheet orientation, thickness, strain history and changes to its  $r$  and  $n$  values under any ratio of applied principal stresses. Shown here are the influences upon limiting formability of: (i) orientation between the principal stress axes and the sheet's rolling direction in 158 increments between 0° and 90°; (ii)  $n$ -values between 0.1 and 0.3; (iii)  $r$ -values between 1.1 and 1.8; (iv) equivalent prestrains from -15 to +15%; (v) sheet thickness between 0.25 and 1.5 mm. The ratio between the in-plane principal stresses is allowed to vary between 0



and  $\pm 1$  for constructing two forming limit diagrams. These forming limit diagrams (FLDs) plot either the limiting in-plane principal engineering strains,  $e_{P1}$  versus  $e_{P2}$ , or the major in-plane and thickness strains,  $e_{P1}$  versus  $e_{P3}$

Faraji et al [26] obtained an LDR of 9 in FE analysis of the multi-stage deep drawing carried out by ABAQUS/explicit FE code. Furthermore, to predict the onset of necking, the forming limit diagram and the forming limit stress diagram were computed and implemented into FE analysis. The best LDRs for each stage were obtained from FE analysis. Experimental tests were conducted based on FE analysis results for comparison purpose. Also, the wall thickness distributions obtained using the finite element method (FEM) was compared with results from several tests.

Choubey et al [27] simulated the deep drawing process with ANSYS 14.0 Software. The die and punch is assumed to be rigid and for the deformable Mild Steel blank, the elasto-plastic analysis is carried out. This way the concern of different process parameters such as coefficient of friction, punch pressure, blank-holder pressure is studied. The main objective of this study is to investigate the effects of Blank-holder pressure (BHP) on the quality of deep drawn product. The effect of BHP variation on failure limits and the limiting drawing ratio in axisymmetric deep drawing operations are studied. Blank material is mild steel and finite element method is used for the simulation. The study includes many aspects that affect the final product.

## CHAPTER 3

### MODELING & SIMULATION

#### 3.1 Modeling

Modeling of the die has been done using the Hyperform die module. Before that the part is modeled in the solidworks and the part has been splitted in half along the XY plane. Then the .iges file is created which is further imported to the hyperform die module.



Fig. 3.1 Die Face Designed in Die Module

The .iges file of the split part is imported to the Hyperform Die Module and geometry clean up is performed to toggle the open edges. After the geometry clean up trim line is created by using create by part option. Then the flat binder is generated and by trimming the binder along the trim line die cavity is created.

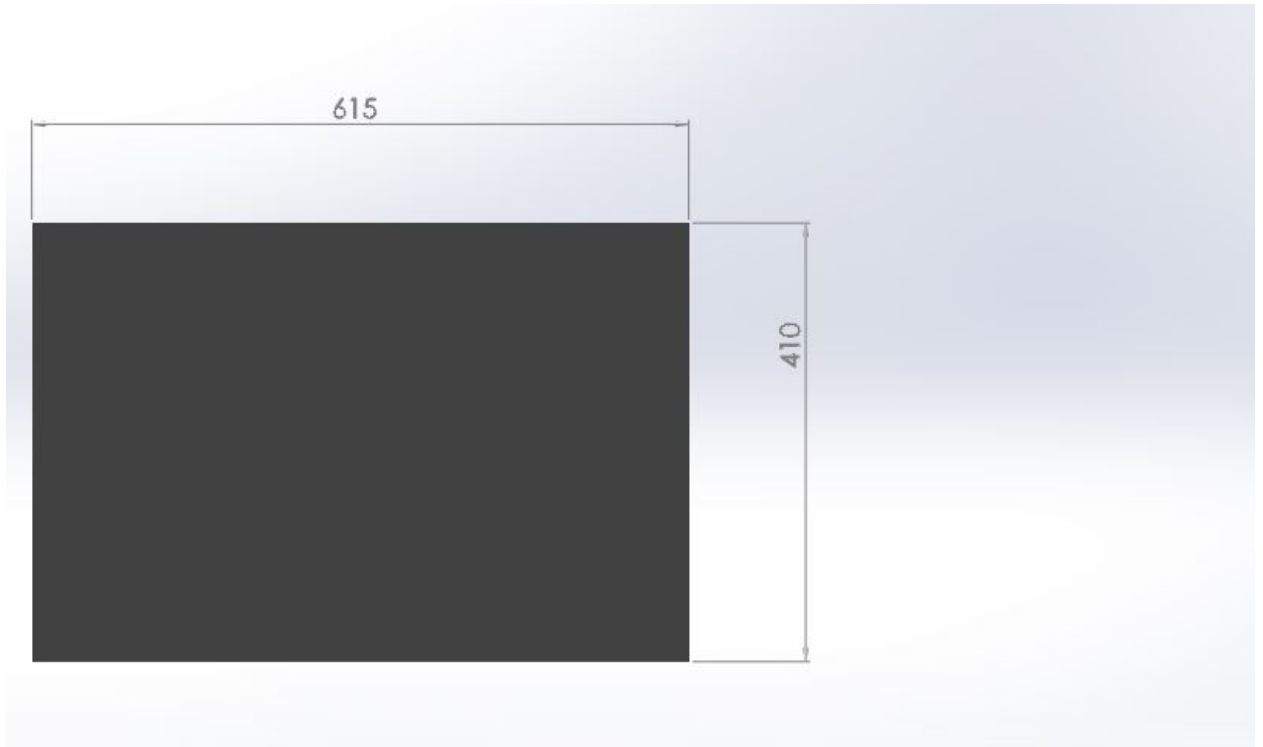


Fig. 3.2 Blank

### 3.2 Simulation

Simulation is performed using Altair HyperForm Radioss which is a complete finite-element-based sheet metal forming simulation framework. Its exclusive process-oriented environment captures the forming process with a suite of highly tailored and configurable analysis and simulation tools. HyperForm delivers a cost-effective solution that allows users to develop an optimal manufacturing process. Two modules of HyperForm Radioss are used, namely Radioss One-Step and Incremental Radioss.

One-Step is a designer friendly model setup for forming feasibility analysis. The solver is very fast and accurate in predicting the blank shape and forming feasibility early in the product development cycle, minimizing downstream formability challenges and associated costs. Its intuitive nesting interface proposes proper blank-sizing, minimizing material scrap in the early stages of the product development process.

Incremental is the module where actual forming simulation takes place. Here, we setup the deep drawing process, either manually through User Process or automatically through Auto Process. It also has function known as Tool Setup that auto generates punch/die and blank holder meshes from the die/punch mesh using input data such as clearance %age and blank holding area. The results are viewed and processed in HyperView.

### **3.2.1 Radioss One-Step Analysis**

In this analysis, CAD geometry, preferably in .igs format is imported and then processed before submitting for feasibility analysis. This processing includes removing holes, if any in the geometry, geometry cleanup, meshing with rigid mesh, autotipping with respect to the drawing direction, which is along z-axis by default, applying material properties, constraints and blank holding pressure.

### **3.2.2 Die Module**

In Hyperform Die module section we can create die face designs for the each step to produce or manufacture a product from a flat blank. In this section we can quickly alter the die surface and repeat the analysis to arrive at the feasible design. We can optimize the die face design and process parameters to avoid the probable defects and land at the feasible and robust process. Hence we can optimize the die structure for maximum tooling life with minimum material to save cost. In this we can also check up for the undercut negative draft in the part with respect to the draw direction. Draw depth based on flat binder can also be calculated. We can develop trim line on the basis of the flanges and addendum.

### **3.2.3 Incremental Forming**

In this module actual simulation of the process takes place that's why it is also known as virtual reality. We can generate binder and punch from the die face designed in the die module section with the suitable percentage clearance between the punch and die. There are two different solvers in this section named as, Incremental RADIOSS and

LS-DYNA. Intuitive interface for designers and engineers for quick model setup. Multistage transfer die or progressive die forming modeling using multistage manager. Supports modeling of single, TWB, Multilayer blanks as shell and solids. Options to create custom process and store it as templates for reuse and share to establish uniform model setup. Fast, Robust, Accurate and Scalable Incremental solver RADIOSS provides quick and best-in-class forming and spring back results. Efficient result interpretation in HyperView with special tools for forming relevant post processing. Simplified interface to setup optimization of process parameters, blank shape, tooling parameter in a stamping process using HyperStudy with HyperForm. Die structure analysis and topology optimization using RADIOSS with Optistruct for maximum tool life and lightweight.

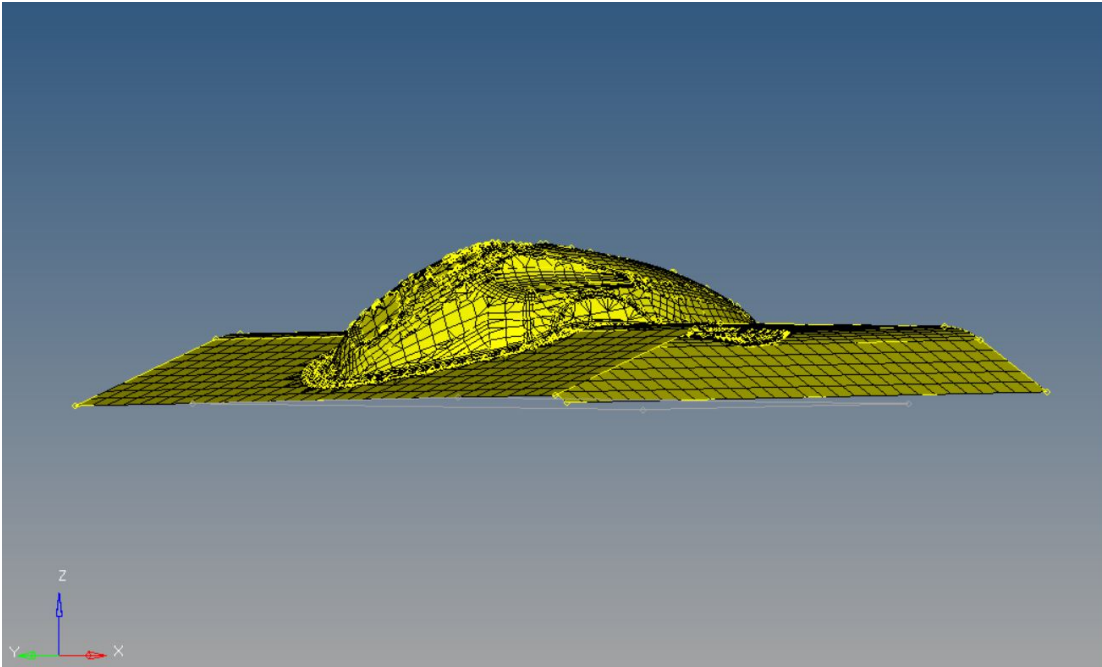


Fig. 3.3 Die with meshing

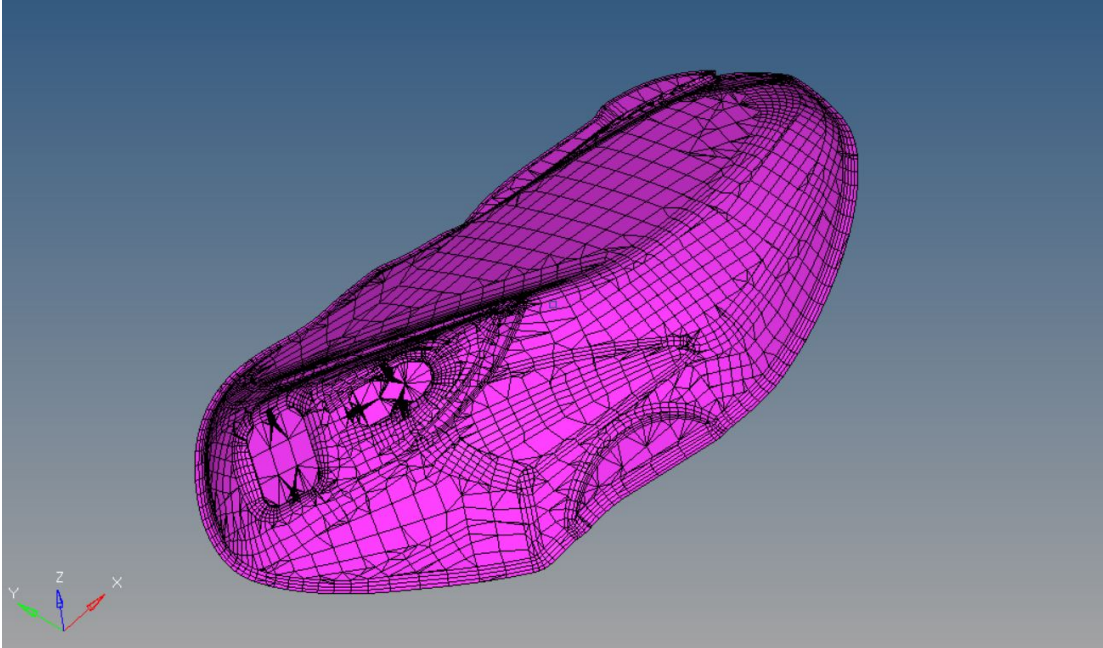


Fig. 3.4 Punch

The die face designed using die module is imported in the incremental RADIOSS. Along with this iges blank file is also imported. Then we go to the mesh>organize>element>components and assign the elements to the die face and blank. First, the die and blank are meshed and then Tool Setup function is used to build and setup the punch and binder from die surface. The Tool Setup function also automatically assigns meshes to punch and binder. The following figure shows the outcome of the Tool Setup function using die-punch clearance as 10%. Die, punch and binder are placed such that they just touch the blank surface.

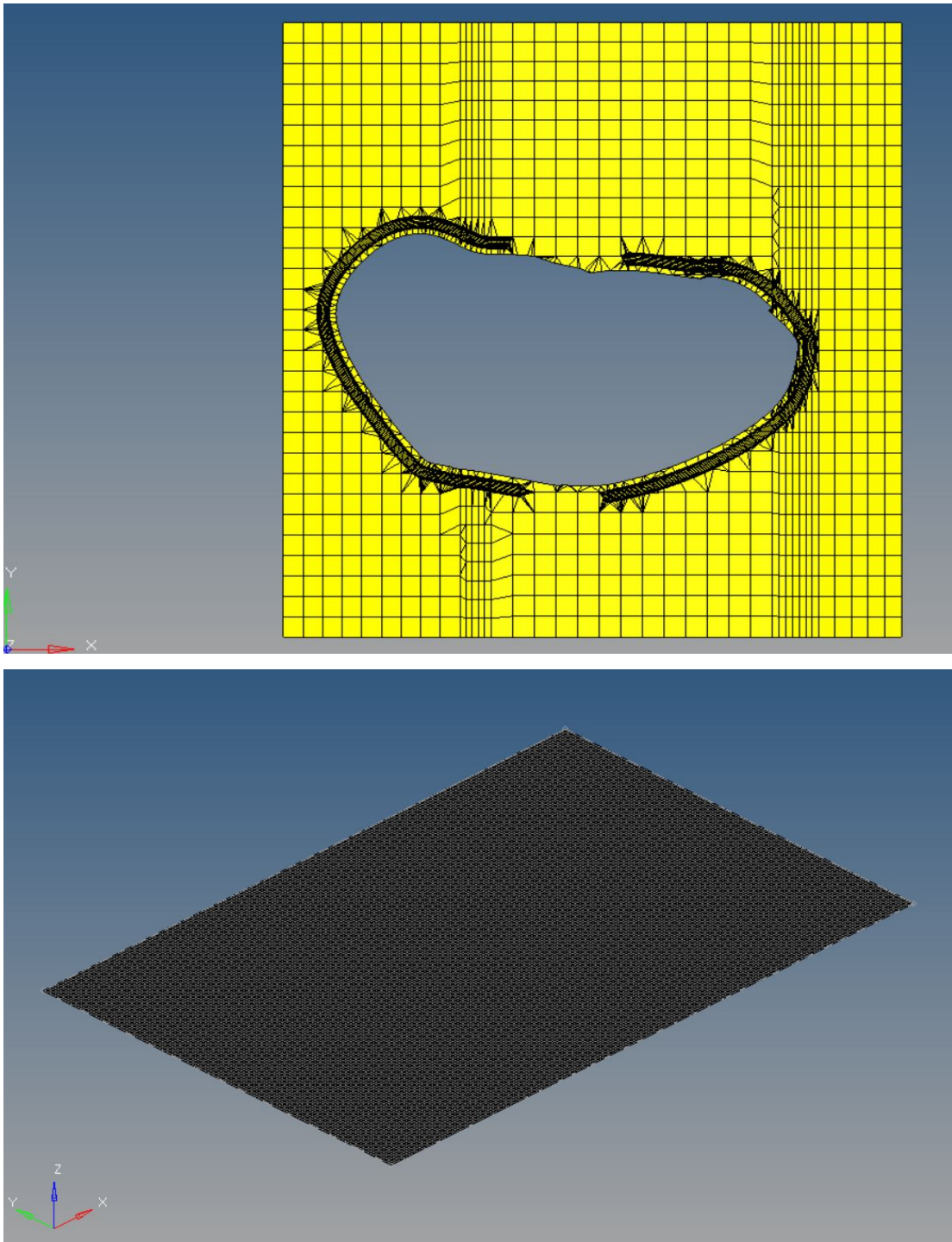


Fig. 3.5 (A) Binder (B) Blank

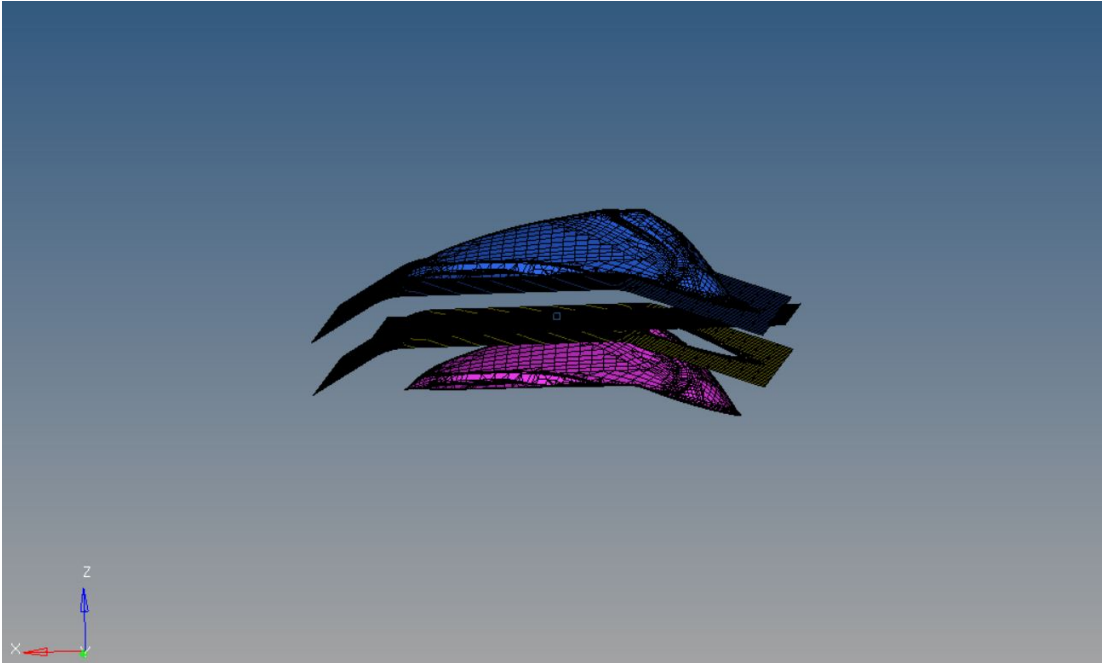


Fig. 3.6 From upside (1) Die (2) Blank (3) Binder (4 )Punch

Die, punch and binder have been assigned rigid meshes known as R-Mesh consisting of four-node shell elements as they are tools and do not need to be analyzed. Binder has been assigned fine B-Mesh or Belytschko-Tsay shells in order to capture the results with accuracy.

After the Tool Setup, User Process is selected in order to finally setup the analysis. We set the material to be used for sheet.

As this is a double action draw, travel and velocity details for punch or die are asked. When we click on calculate distance, then it will calculate the travel details. These calculated are automatically fed, with respect to the condition that all other tools just touch the blank. We can also change these values according to our requirements.



The final part is drawn in by using 200 KN blank holding force and draw depth of 78mm. The frictional coefficients between various surfaces are as given below:

Table 3.1 Friction values

S.No.	Contact Surfaces	Coefficient of friction
1	Die-Blank	0.125
2	Binder-Blank	0.125
3	Punch-Blank	0.125

Then we click on Apply to apply these values to the model and Run to run the analysis using Radioss. After the completion we go to utilities and click on the report generator. Then select the animation files written by the software which have.rad format and click on the view results. We can also change the number of animation frames. The results are displayed in the Hyperview and can be exported in .H3D format or .html format. In h3d there is video file whereas in .html images are displayed.

## CHAPTER 4

### EXPERIMENTAL WORK

#### 4.1 Materials Selection

Chemical composition of CRDQ and Interstitial Free steels used for experimental work is determined by the spectrometer. The SPECTROTEST is a mobile arc spark spectrometer ideal for many applications in the metal producing, processing, and recycling industries. This mobile metal analyzer flaunts its superior performance especially when exact metal analysis is required, when materials are difficult to identify or when there is a large number of samples to be tested.

The complex arc spark spectrometer design offers many ergonomic advantages for safe and fatigue-free onsite operation. The light, thin probe is quickly converted between arc excitation and spark excitation (arc spark OES). A probe with an integrated UV optic is available for special measuring applications; in its newest version it can also be utilized with arc excitation.

This arc spark spectrometer is even able to identify low alloy steel with the carbon content during the rapid arc excitation mode. In spark mode, the SPECTROTEST's analysis of carbon phosphorous and sulfur are potential applications in addition to the identification of duplex steels using the nitrogen content.

Table 4.1: Chemical composition of the CRDQ & IF steel used (by weight %)

Elements	C	Si	Mn	Ni	Cr	Cu	V	Al	Ti	S	P
CRDQ	0.053	.018	0.076	0.039	0.037	0.022	0.036	0.018	0.045	0.020	0.016
IF Steel	0.004	.002	0.112	0.012	0.012	0.009	0.017	.0048	0.025	0.009	0.017

#### **4.1.1 Interstitial Free steel**

These are also known as the extra deep draw steel. These are steels from which carbon and nitrogen have been reduced to extremely low levels (less than 0.005%). After vacuum degassing, titanium is added to react with any carbon or nitrogen in solution. Titanium reacts preferentially with sulfur so the stoichiometric amount of titanium that must be added to eliminate carbon and nitrogen is

$$\%Ti = (48/14)(\%N) + (48/32)(\%S) + (48/12)(\%C)$$

#### **4.1.2 Cold Rolled Deep Quality**

Cold rolled steel offers a wide variety of properties including ease of formability, a smooth and clean surface that's why there are mostly used in automobiles, furniture and other appliances. The formability of products is determined by annealing. Because cold rolling significantly increases material hardness, making forming difficult, annealing is performed to improve ductility by inducing a recrystallized structure in the steel. Annealed coils are lightly rolled by the skinpass mill to prevent a defect called stretcher strain, improve strip shape, and adjust mechanical properties. Skinpass rolling is also used to produce dull finish and bright finish products. Depending upon the application the process of production and composition of the cold rolled steel is changed.

## 4.2 Determination of tensile properties

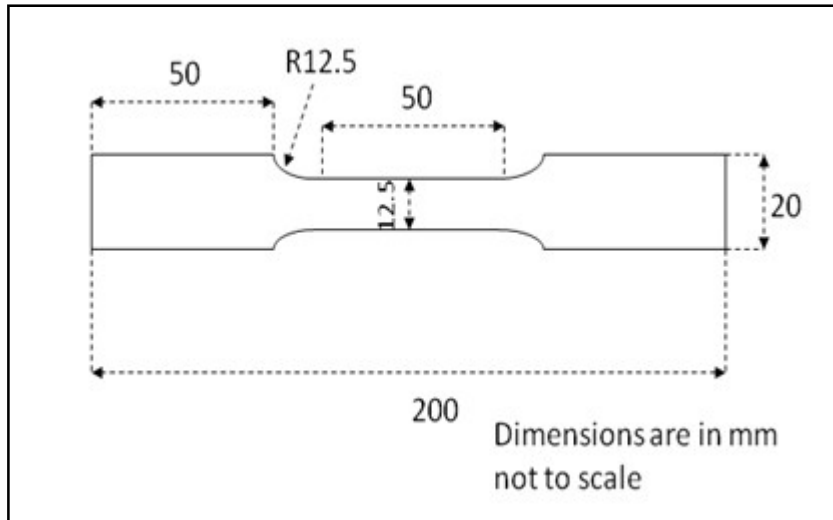


Fig. 4.1: Dimensions of Tensile specimen (ASTM E8)

The specimens as per ASTM standard E8M as shown in Fig. 4.1 are used for tensile testing. The specimens were prepared in three directions with the length parallel ( $0^{\circ}$ ), diagonal ( $45^{\circ}$ ) and perpendicular ( $90^{\circ}$ ) to the rolling direction of the sheet.



Fig. 4.2 50kN-UTM-table top in Metal Forming Lab. at DTU

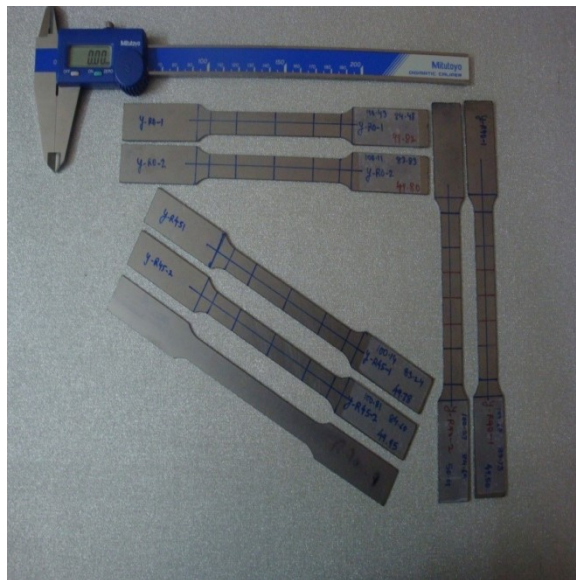


Fig. 4.3 Tensile test specimens in 0°, 45° and 90° to rolling direction as per ASTM E8M standard.

The specimens are tested in uniaxial tension on UTM table top (Fig. 4.2) at a constant cross head speed of 5 mm/min. The tested and untested tensile samples are shown in Figure. Load elongation data was obtained for all the tests which were converted into engineering stress strain curves. The standard tensile properties such as yield stress, ultimate tensile stress, uniform elongation and total elongation are determined from the stress- strain data.

The point corresponding to max stress was taken as the UTS and the stress at 20% offset is taken as the YS. The total elongation is measured using an initial gauge length of 50.8 mm.

The strain hardening behavior can be described using the Holloman's equation.

$$\sigma = K\varepsilon^n$$

Where  $\sigma$ =true stress,  $\varepsilon$ =true strain,  $n$ =strain hardening exponent,  $K$ =strength coefficient.

For determining the  $n$  value of these sheets, the engineering stress strain data were converted into true stress-true strain curves using the following equations.

$$\sigma = s(1 + e)$$

$$\varepsilon = \ln(1 + e)$$

Where  $s$  = engineering stress and  $e$ = engineering strain.

The log true stress and log true strain values are calculated in the uniform plastic deformation range (between YS and UTS) and using linear regression (least square method) a best fit was plotted. The slope of this line gives  $n$  value and Y- intercept gives  $\log K$ .

### **4.3 Mechanical Properties of Materials**

Various mechanical properties of the materials which are determined from the data obtained from the tensile test of the specimens are displayed in the table 4.2.

Table 4.2: Different Mechanical properties of CRDQ & IF steel

UTS	Yield Stress	EL%	Hardness(HRB)	Anisotropy (r)	Strain hardening coefficient (n)
342.74 N/mm <sup>2</sup>	186.89 N/mm <sup>2</sup>	44.20	69-70	1.5	.22
249 N/mm <sup>2</sup>	110.67 N/mm <sup>2</sup>	47.3	30	2	.28

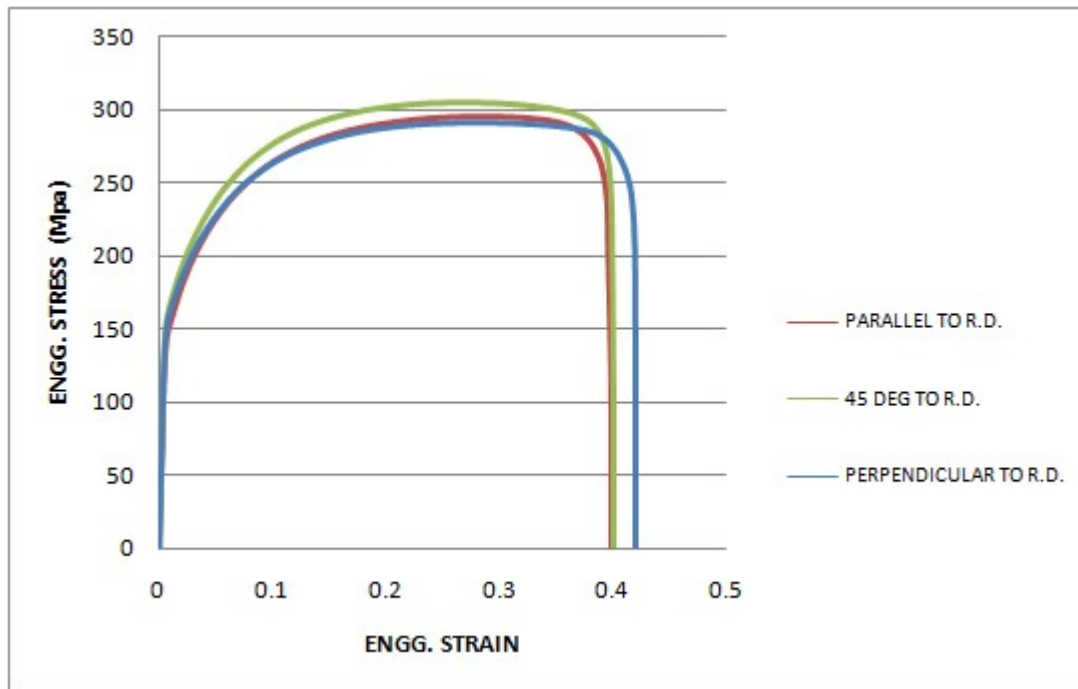


Fig. 4.4 Engineering Stress-Strain Curve of CRDQ Steel

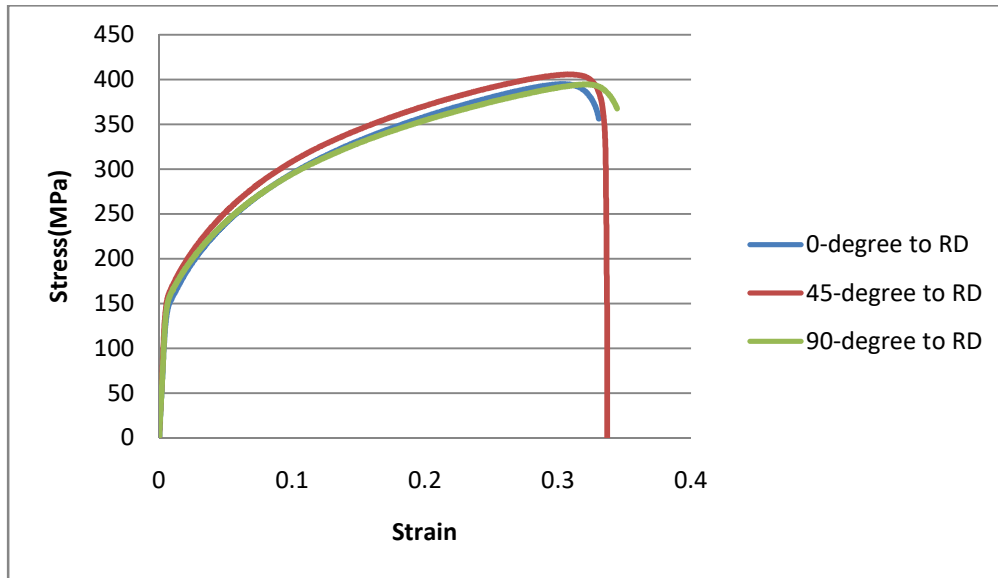


Fig. 4.5 True Stress-strain curve CRDQ Steel

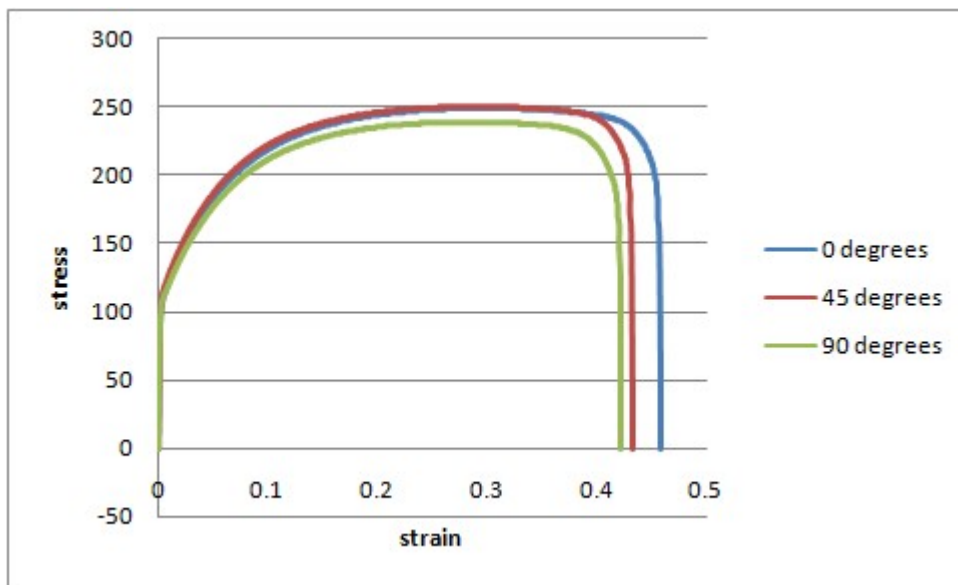


Fig. 4.6 Engineering stress (MPa)-strain curve of IF Steel



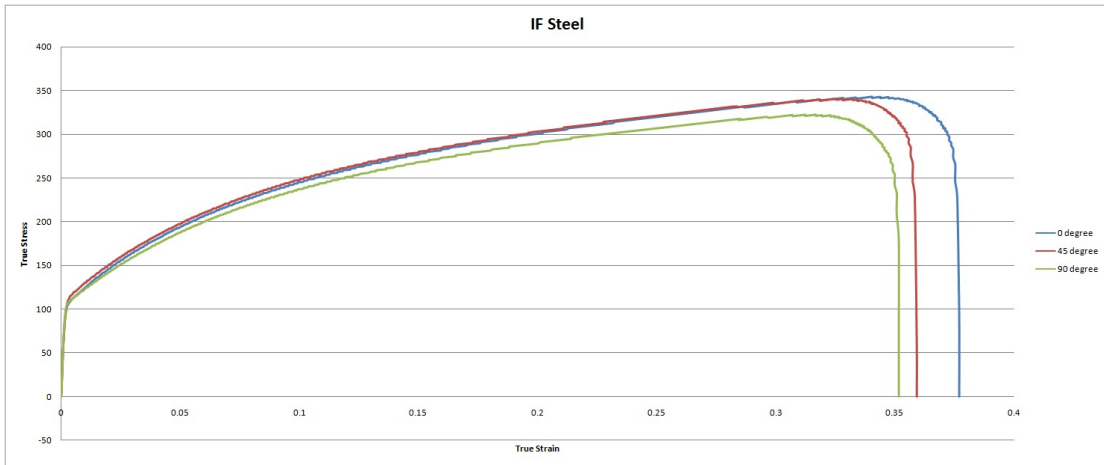


Fig. 4.7 True stress (MPa) – strain curve IF Steel

## CHAPTER 5

### RESULTS AND DISCUSSION

#### 5.1 Introduction

In this chapter, deep drawing process simulated in hyperform has been explained. Hyperform was used to predict percentage thinning, plastic strain and forming limit diagram. There are four cases discussed in this chapter for two materials i.e, CRDQ and IF steels and two thickness, i.e, 0.8mm and 1.2mm.

#### 5.2 Problem Formulation

The figure 5.1 represents the deformed blank and an unsuccessful attempt of drawing. There have been many trial run computed at different blank holding forces but due to insufficient forces wrinkling was evident and slipping was also seen due to which simulation was terminated in between.

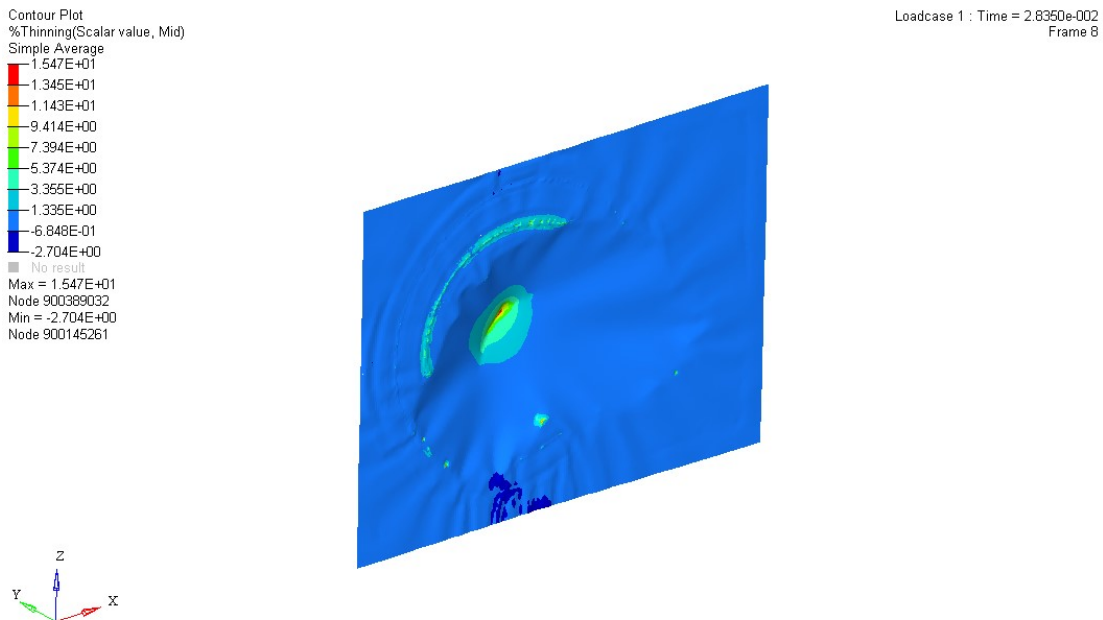
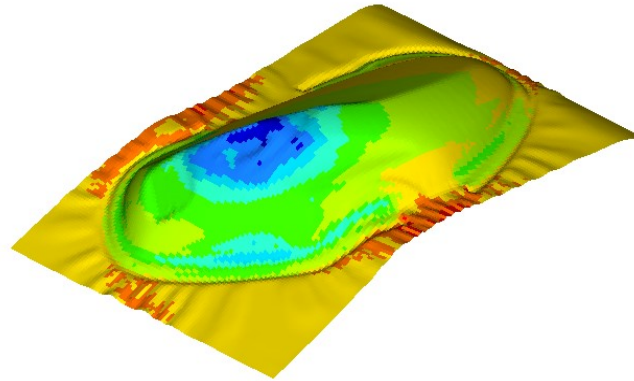


Figure 5.1 An incomplete draw part under 25 KN binder force.

**Case I: Material used IF steel and thickness is 0.8mm**

Contour Plot  
Thickness(Scalar value, Mid)  
8.777E-01  
8.454E-01  
8.131E-01  
7.807E-01  
7.484E-01  
7.160E-01  
6.837E-01  
6.514E-01  
6.190E-01  
5.867E-01  
■ No result  
Max = 8.777E-01  
SHELL 17010  
Min = 5.867E-01  
SHELL 23073

Loadcase 1 : Time = 5.9401e-002  
Frame 11



Contour Plot  
%Thinning(Scalar value, Mid)  
Simple Average  
2.612E+01  
2.237E+01  
1.861E+01  
1.486E+01  
1.111E+01  
7.351E+00  
3.597E+00  
-1.571E-01  
-3.911E+00  
-7.665E+00  
■ No result  
Max = 2.612E+01  
Node 22304  
Min = -7.665E+00  
Node 11185

Loadcase 1 : Time = 5.9401e-002  
Frame 11

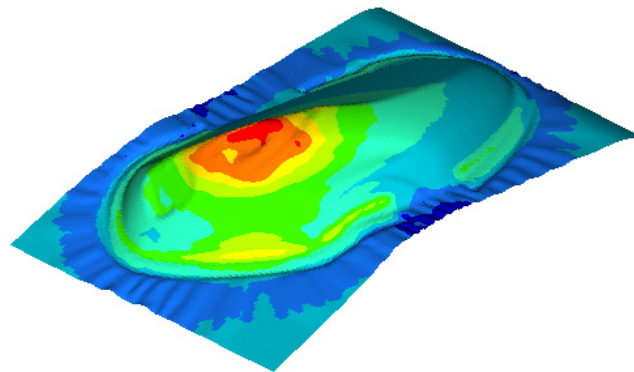


Fig. 5.2 (A) Variation of the thickness throughout the blank. (B) Percentage thinning contour of 0.8mm

As it can be clearly seen in the thickness variation contour that the blank thickening takes place in the flange region of the blank. The shells in which the maximum and minimum value of the thickness occurs are shown in the diagram. According to the percentage thinning contour the simple average thinning is 26.16% which is

restrained to the very little area. Further we can observe the forming limit diagram if there any sign of the failure due to excess thinning of the blank.

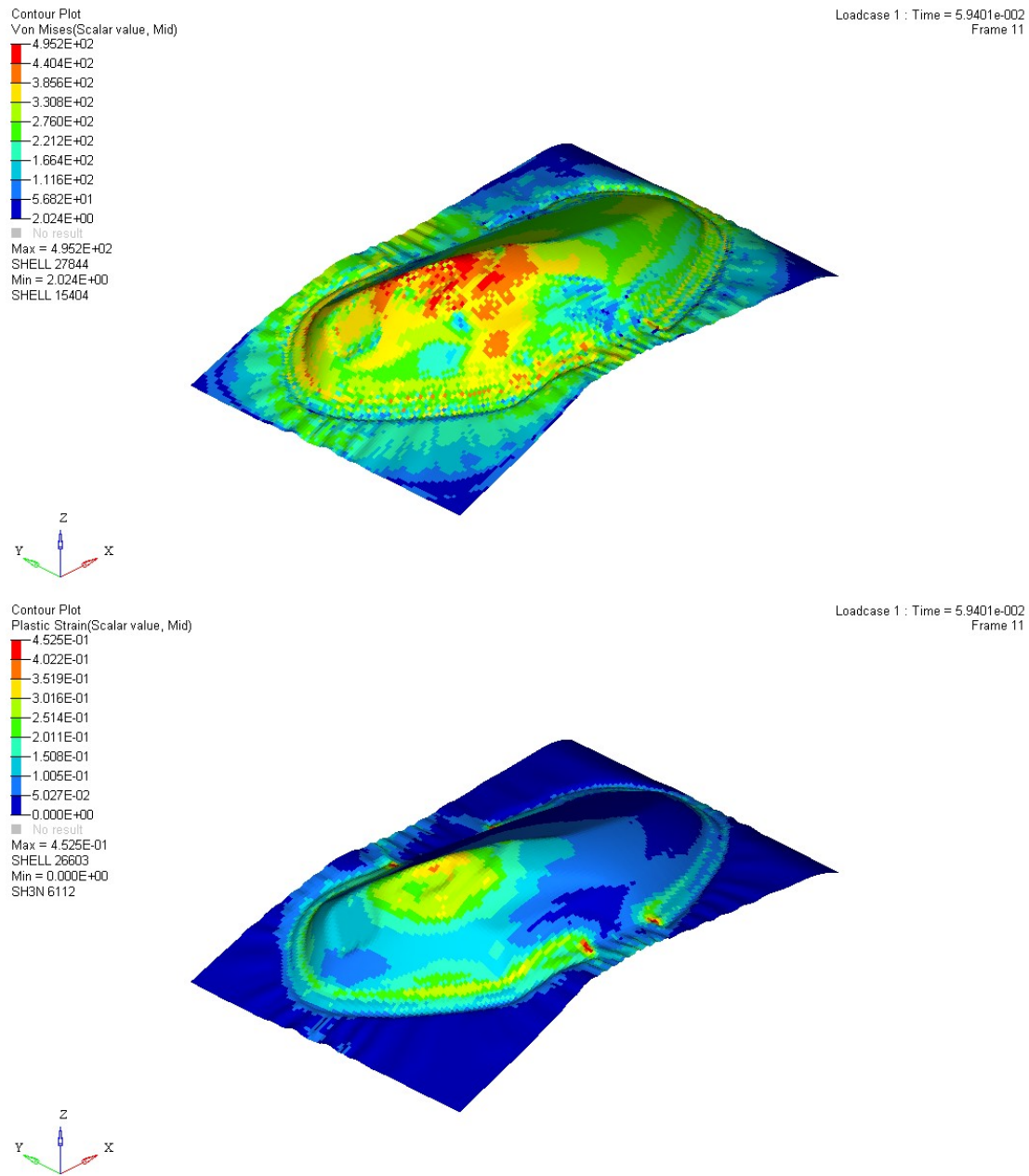


Fig. 5.3 (A) Contour plot of the Von- Mises stresses. (B) Average plastic strain contour plot.

The Von –Mises stress and plastic strain values of the 0.8 mm thick sheet is shown in the figure 5.3. From the comparison between the thickness contour plot and von–

mises stress plot, it is clearly that the stresses and plastic strain are maximum in the region where there is maximum thinning is occurring. This is due to the intricate contour in the part.

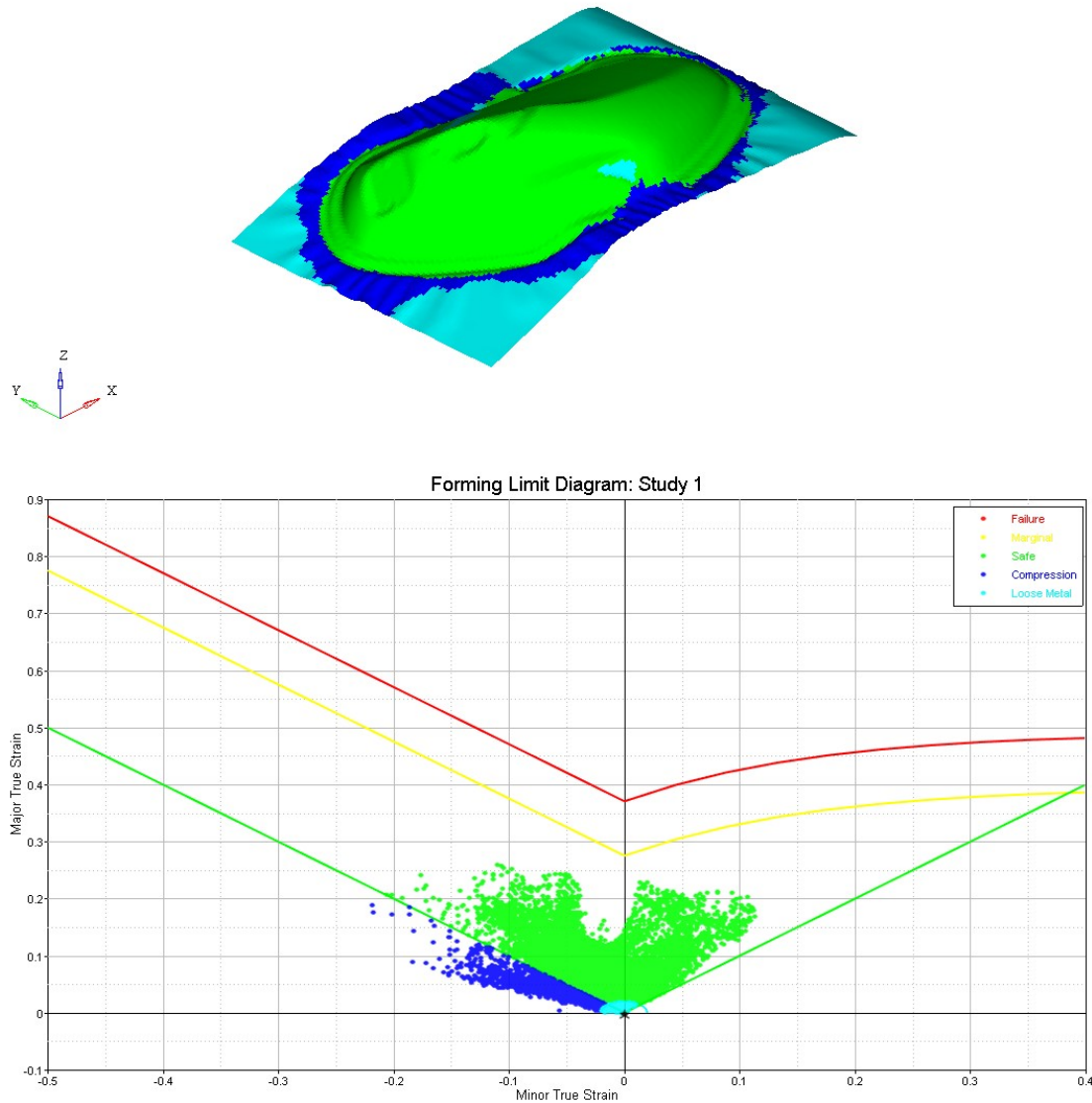
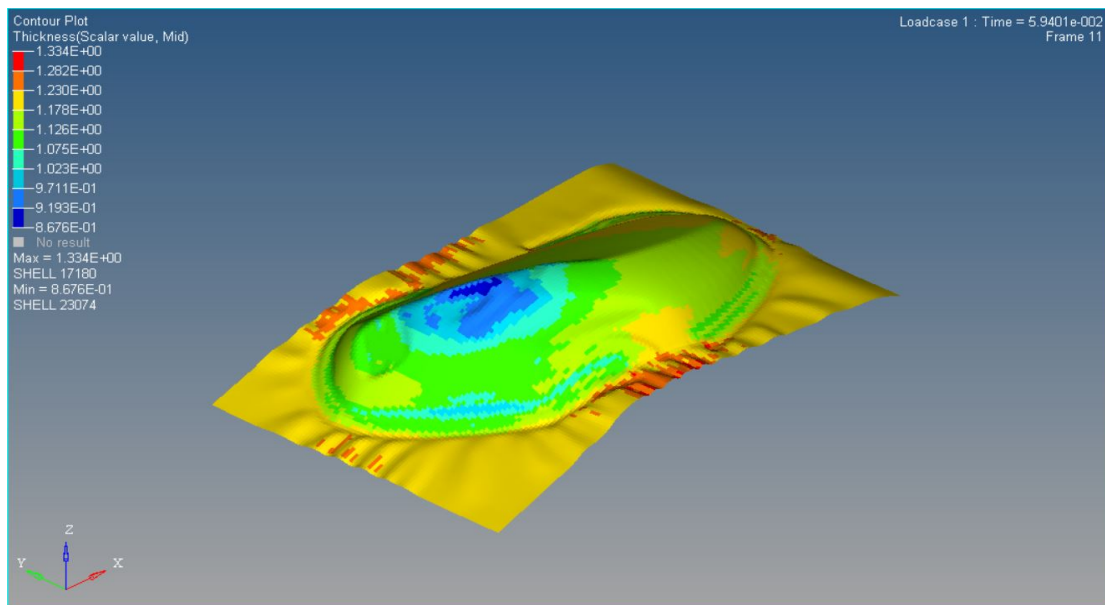


Fig. 5.4 Forming limit diagram of the 0.8 mm thick IF Steel blank.

As displayed in the forming limit diagram above there are no chances of the failure of any area of the blank. Majority of the portion of the blank is in the safe region. Even

the small fraction of area which is having maximum thinning percentage has no chances of failure. The region indicated by the blue color is under compression and the part of the flange region. All the portion of the flange lies in the second quadrant which means that it is subjected to the positive major strain and negative minor strain. The maximum thickening occurs in the portion which is displayed as loose metal in the forming limit diagram.

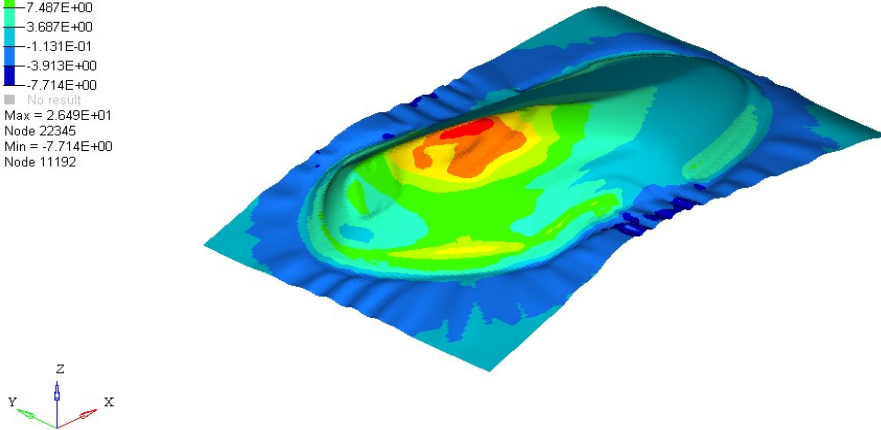
***Case II: Material used IF steel and thickness is 1.2mm***



(A)

Contour Plot  
 %Thinning(Scalar value, Mid)  
 Simple Average  
 2.649E+01  
 2.269E+01  
 1.889E+01  
 1.509E+01  
 1.129E+01  
 7.487E+00  
 3.687E+00  
 -1.131E-01  
 -3.913E+00  
 -7.714E+00  
 No result  
 Max = 2.649E+01  
 Node 22345  
 Min = -7.714E+00  
 Node 11192

Loadcase 1 : Time = 5.9401e-002  
 Frame 11



(B)

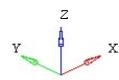
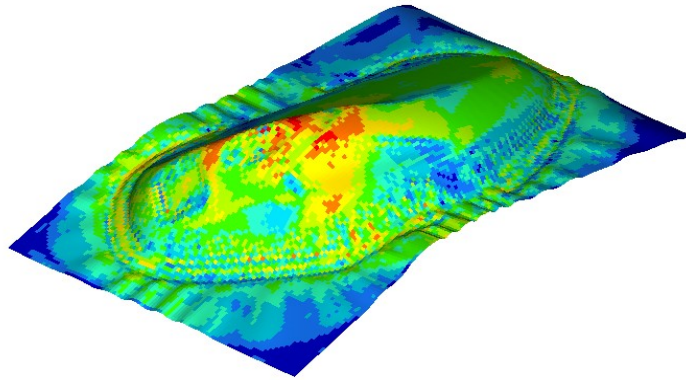
Fig. 5.5 (A) Contour plot of the variation of the scalar value of thickness 1.2 mm thick blank. (B) Percentage thinning contour plot of 1.2 mm thick IF Steel blank.

With increasing the thickness of the blank there is slight increase in the simple average percentage thinning. As shown in the percentage thinning contour of the 1.2 mm thick blank the maximum thinning percentage is 26.49% whereas in case of 0.8mm thick blank it was 26.12%. Scalar values of the maximum and minimum percentage thickness may be varying from the percentage given by the simple average thinning plot.

The value of the maximum von-mises stress is also increase with increasing the thickness of the blank. The maximum value of the stress in 1.2mm blank is 497.4MPa which is 495MPa in case of 0.8 mm thick blank. On the other hand, the value of the simple average plastic strain decrease in 1.2mm thick blank as shown in the figure 5.6. The strain value which is 0.45 in 0.8mm case reduces to .41 in 1.2mm thick blank. We can also plot the tensor plot for the different type of the strain like maximum in-plane strain etc.

Contour Plot  
 Von Mises(Scalar value, Mid)  
 4.974E+02  
 4.423E+02  
 3.871E+02  
 3.320E+02  
 2.769E+02  
 2.218E+02  
 1.667E+02  
 1.115E+02  
 5.642E+01  
 1.302E+00  
 No result  
 Max = 4.974E+02  
 SHELL 23073  
 Min = 1.302E+00  
 SHELL 18408

Loadcase 1 : Time = 5.9401e-002  
 Frame 11



Contour Plot  
 Plastic Strain(Scalar value, Mid)  
 Simple Average  
 4.177E-01  
 3.713E-01  
 3.249E-01  
 2.784E-01  
 2.320E-01  
 1.856E-01  
 1.392E-01  
 9.281E-02  
 4.641E-02  
 0.000E+00  
 No result  
 Max = 4.177E-01  
 Node 25781  
 Min = 0.000E+00  
 Node 2

Loadcase 1 : Time = 5.9401e-002  
 Frame 11

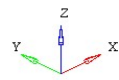
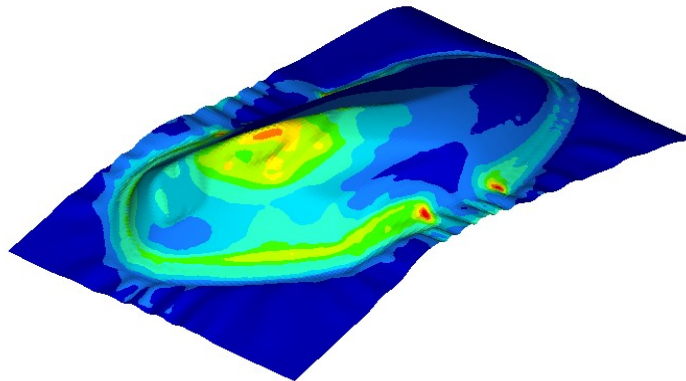


Fig. 5.6 Contour plot of the Von-mises stresses and plastic strain of 1.2mm thick IF Steel blank.

Even after the higher values of the percentage thinning relatively to the 0.8mm blank, the chances of failure due to tearing and wrinkle tendency of the part are still very less. The FLD of the 1.2mm blank is shown in the figure 5.7.



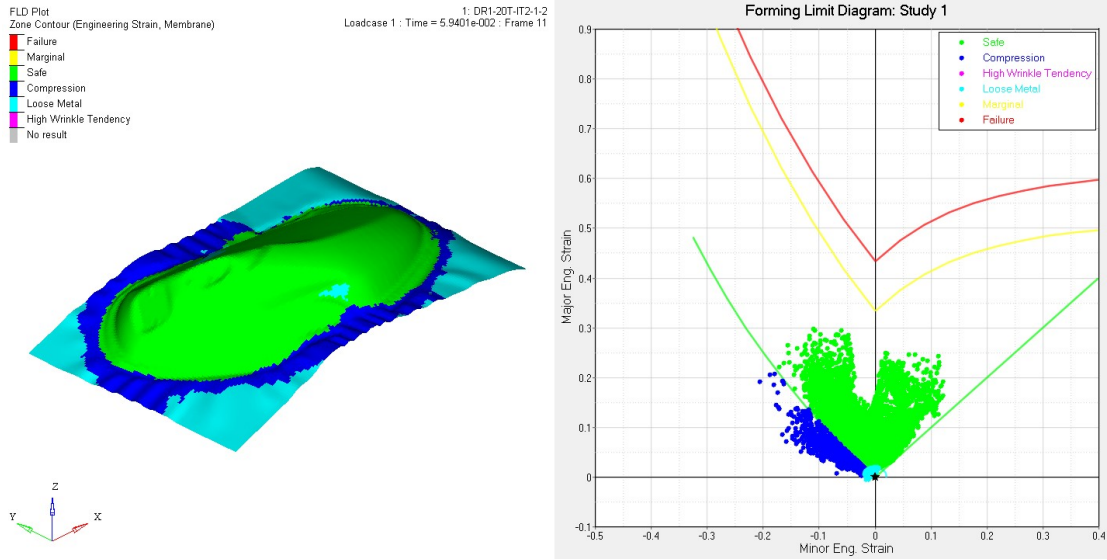


Fig.5.7 FLD of the 1.2mm thick IF Steel blank.

**Case III: Material used CRDQ steel and thickness is 0.8mm**

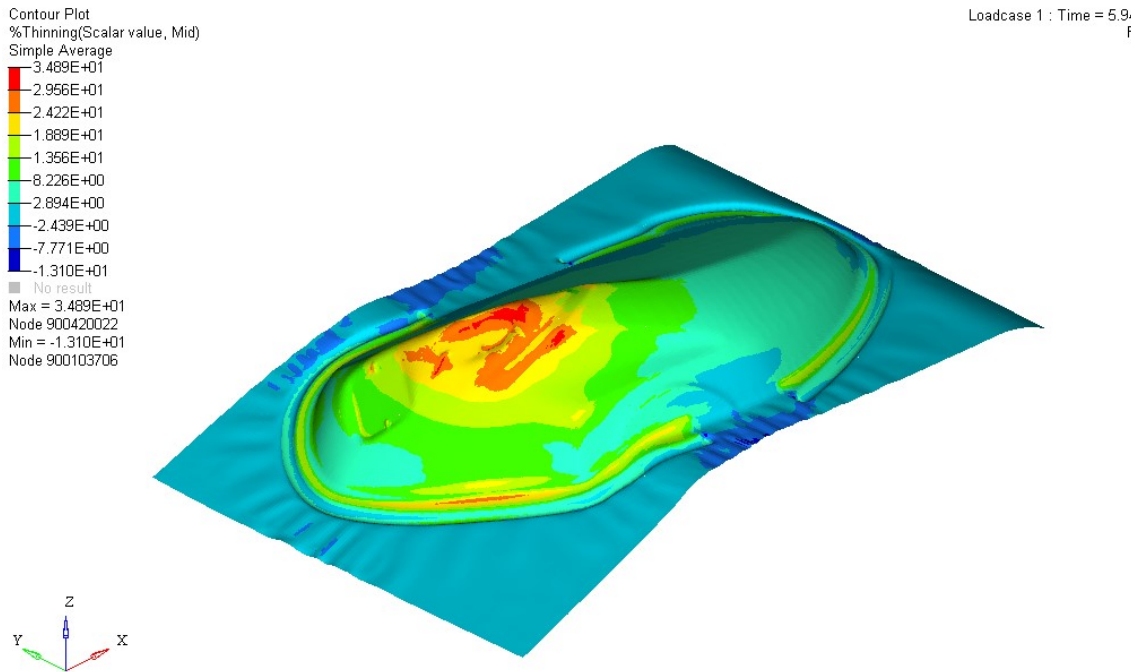


Fig. 5.8 Percentage Thinning 0.8mm CRDQ Steel Blank

Contour Plot  
 Plastic Strain(Scalar value, Mid)  
 Simple Average

7.588E-01
6.745E-01
5.902E-01
5.059E-01
4.216E-01
3.373E-01
2.529E-01
1.686E-01
8.431E-02
0.000E+00

■ No result  
 Max = 7.588E-01  
 Node 900389069  
 Min = 0.000E+00  
 Node 100000001

Loadcase 1 : Time = 5.9  
 f

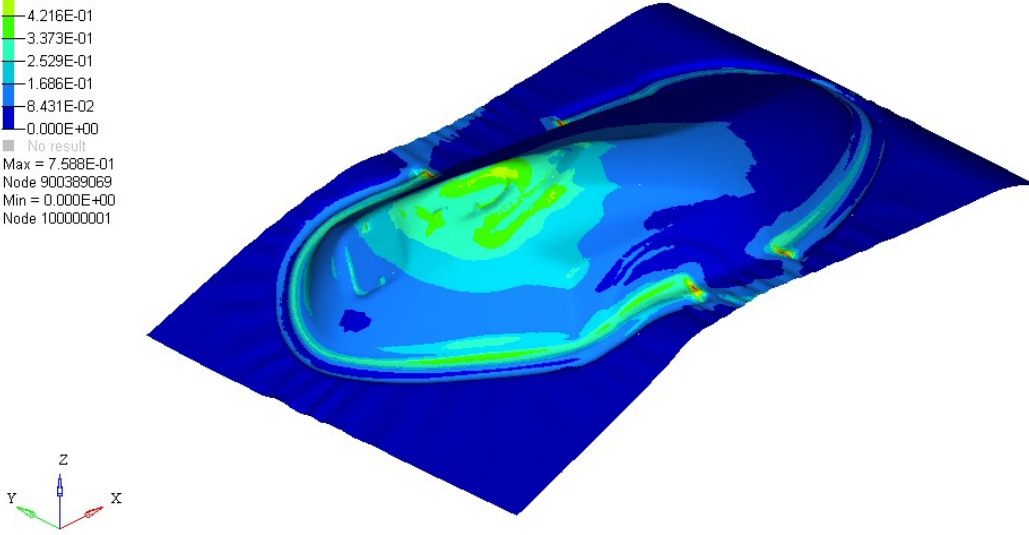


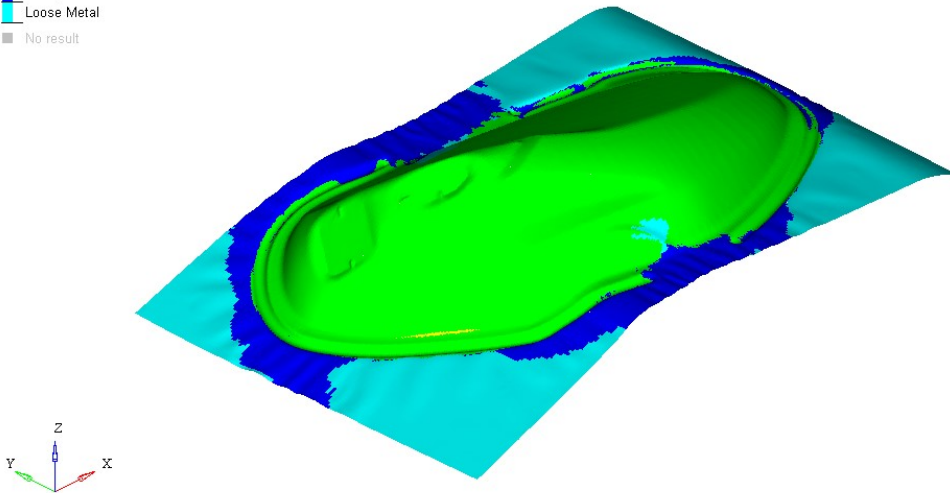
Fig. 5.9 Plastic Strain 0.8mm CRDQ Steel

FLD Plot  
 Zone Contour (True Strain, Mid)

Failure
Marginal
Safe
Compression
Loose Metal

■ No result

Loadcase 1 : Time = 5.9401e-002  
 Frame 11



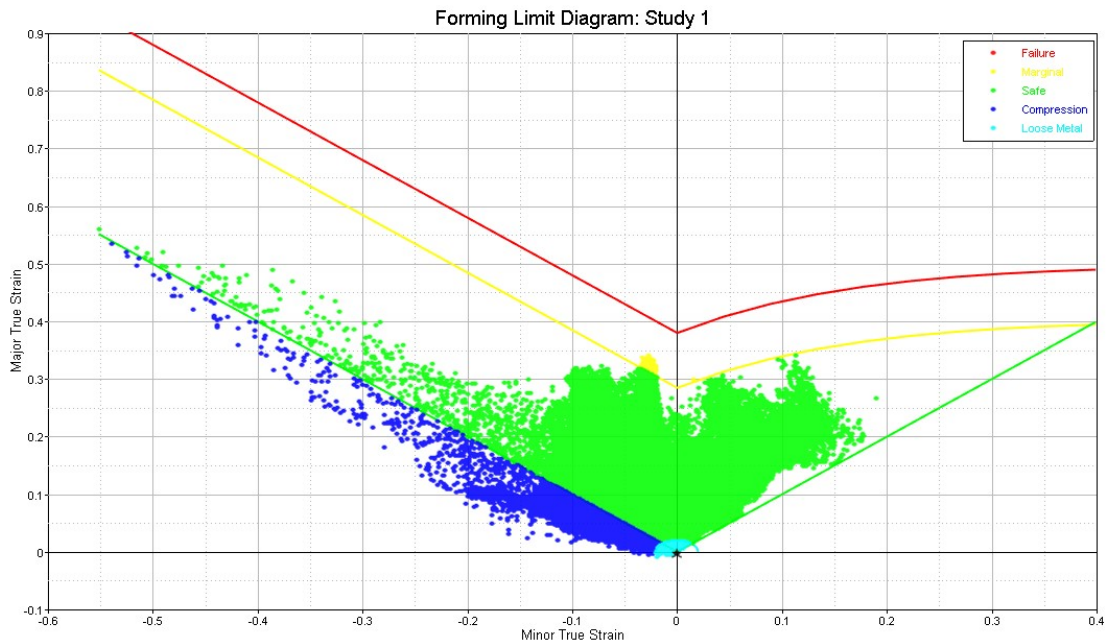


Fig. 5.10 Forming Limit Diagram 0.8 mm thick CRDQ Steel Blank

From the simulation results of deep drawing of fuel tank , for the case of CRDQ steel with thickness .8 mm the maximum percentage thinning came out to be 34.89% and minimum value of percentage thinning is -13.10%. The plastic strain remains confined to the upper limit of the .07588. It is evident from these results that despite increase in percentage thinning value of CRDQ steel from case of IF steel , the FLD diagrams shows that there is no failure of material although there are some wrinkles developed but these are in the flanges which would not be the part of final component as they would be trimmed in finishing stages.

**Case IV: Material used CRDQ steel and thickness is 1.2mm**

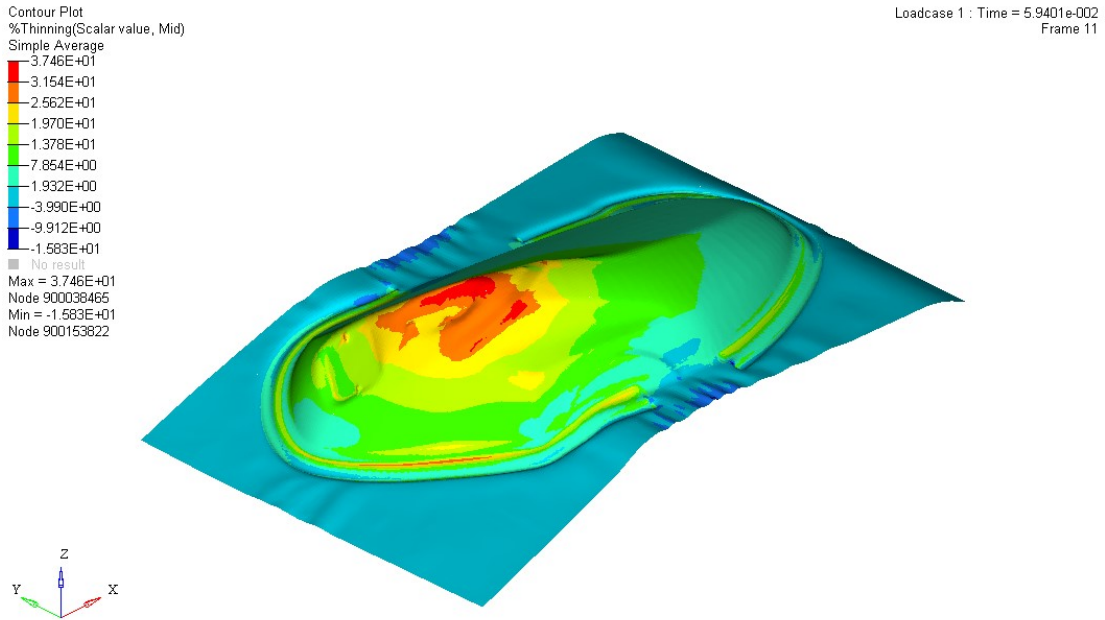


Fig. 5.11 Percentage thinning of 1.2mm thick CRDQ Steel Blank

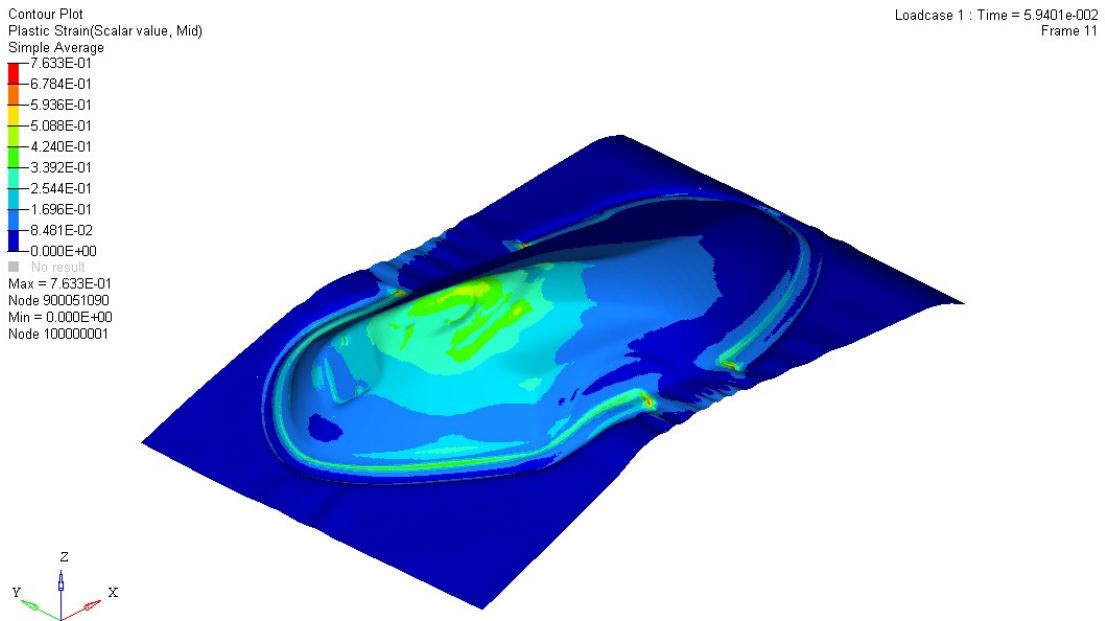


Fig. 5.12 Plastic strain 1.2mm CRDQ Steel

FLD Plot  
 Zone Contour (True Strain, Mid)

- Failure
- Marginal
- Safe
- Compression
- Loose Metal
- No result

Loadcase 1 : Time = 5.9401e-002  
 Frame 11

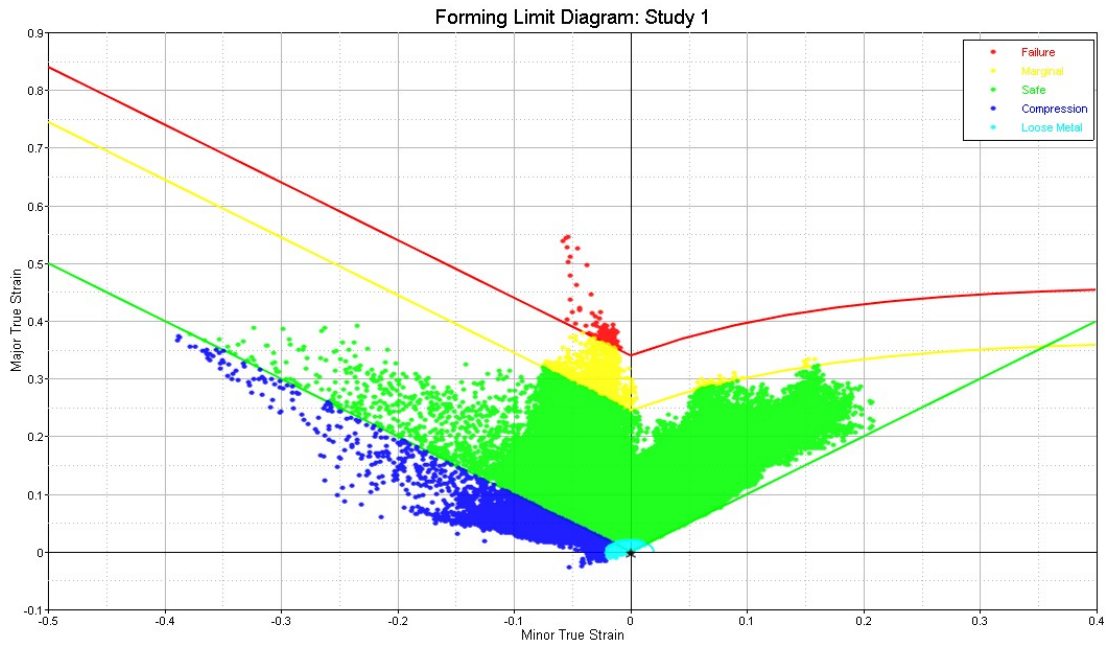
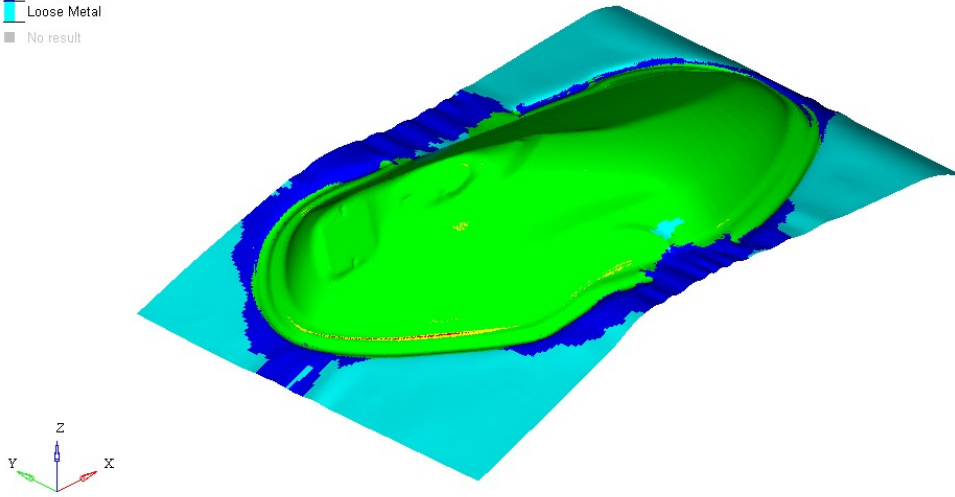


Fig. 5.13 FLD 1.2mm thick CRDQ Steel Blank

The simulation results of deep drawing of fuel tank , for the case of CRDQ steel with thickness 1.2 mm exhibits the maximum percentage thinning of 37.46% and value of percentage thickening of 18.83%. The plastic strain remains confined to the upper limit of the .07633. With increase in thickness of blank from .8 to 1.2 the percentage thinning also increases and this trend was also visible in the case of IF steel for increase in thickness.

## CHAPTER 6

### CONCLUSION AND FUTURE SCOPE

#### 6.1 Conclusion

This dissertation work has been attempted to understand the deep drawing process through simulation only. Experimental work has not been done as the Altair Hyperform gives us the FLD, which are broadly used to predict failure in forming processes. Radioss One-Step optimised the initial blank and helps in blank nesting which further increase the material utilization during the blanking process. Initially the product is showing very high wrinkling tendency due to the insufficient binder force. With increasing the binder force the wrinkling keep on decreasing. With increase in thickness of the blank the percentage thinning and von-mises stresses also increase unlike the plastic strain which decreases with increasing thickness. Even the final drawn product is having slightly higher value of the percentage thinning but forming limit diagram is showing no sign of failure. Hence, the little extra thinning is tolerable in the final product. CRDQ steel shows more percentage thinning as compared to IF for same thickness of blank although they follow the same trend of increase of percentage thinning with increase in thickness of blank and and plastic strain also increase as we move from IF to CRDQ steel for same thickness of blank.

#### 6.2 Future Scope

- In future studies springback effect can be taken into account.
- Die stress analysis can also be performed future studies.
- Temperature effects during the forming process can be taken into account.
- Varying binder force can be applied to this analysis.
- Different friction values can be used in analysis.

## REFERENCES

- [1] Zein H., Sherbiny M. EL., "Thinning and Spring Back Prediction of Sheet Metal in the Deep Drawing Process", *Materials and Design* 53 (2014) 797–808.
- [2] Anaraki A.P., Shahabizadeh M., Babae B., "Finite Element Simulation of Multi-Stage Deep Drawing Processes & Comparison with Experimental Results", *World Academy of Science, Engineering and Technology* 61 2012.
- [3] Kumar B.S., Patil D.C., Gowda R.D., "Finite Element Simulation of Sheet Metal Deep Drawing Using Explicit Code and Result Validation", (IRJET) e-ISSN: 2395-0056 Volume: 02 Issue: 06 , Sep-2015.
- [4] Arab N., "Experimental and Simulation Analysis of Deep Drawing Cylindrical Cup Process", *Merit Research Journal of Petroleum, Geology and Mining* Vol. 1 (1) pp. 001-008, August, 2013.
- [5] Han J., Yamazaki K., Makino S., "Optimization of Deep Drawing Process for Circular Cup Forming", *10th World Congress on Structural and Multidisciplinary Optimization* May 19 -24, 2013.
- [6] Hill, Rodney. "The mathematical theory of plasticity". Vol. 11. Oxford university press, 1998.
- [7] Chung, S. Y., and H. W. Swift. "Cup-drawing from a flat blank: part I. Experimental investigation." *Proceedings of the institution of mechanical engineers* 165.1 (1951): 199-211.
- [8] Chung, S. Y., and H. W. Swift. "Cup-drawing from a flat blank: part II. Analytical investigation." *Proceedings of the institution of mechanical engineers* 165.1 (1951): 211-215
- [9] Lankford, W. T., S. C. Snyder, and J. A. Bauscher. "New criteria for predicting the press performance of deep drawing sheets." *Trans. ASM* 42 (1950): 1197-1232.
- [10] El-Sebaie, M. G., and P. B. Mellor. "Plastic instability conditions in the deep-drawing of a circular blank of sheet metal." *International Journal of Mechanical Sciences* 14.9 (1972): 535-540.



- [11] Darendeliler, H., and B. Kaftanoglu. "Deformation analysis of deep-drawing by a finite element method." *CIRP Annals-Manufacturing Technology* 40.1 (1991): 281-284.
- [12] Yang, D. Y., and H. S. Lee. "Analysis of three-dimensional deep drawing by the energy method." *International journal of mechanical sciences* 35.6 (1993): 491-516.
- [13] Lee, C. H., and Shiro Kobayashi. "New solutions to rigid-plastic deformation problems using a matrix method." *Journal of Engineering for Industry* 95.3 (1973): 865-873.
- [14] Saran, Michal J., and Alf Samuelsson. "Elastic-viscoplastic implicit formulation for finite element simulation of complex sheet forming processes." *International journal for numerical methods in engineering* 30.8 (1990): 1675-1697.
- [15] Seo, Young. "Simulation beats trial-and-error." *Metal Forming(USA)* 36.5 (2002): 32-34.
- [16] Jain, N., Shi, X., Ngaile, G., Altan, T., Pax, B., Harman, B., & Homan, G. (2003). "Simulation Confirms Deep Drawn Die Design". *Metal Forming Magazine*, 51-56.
- [17] Keeler, S. P.: Plastic instability and fracture in sheet stretched over rigid punches, Thesis, Massachusetts Institute of Technology, Boston, MA 1961.
- [18] Keeler, Stuart Philip, and Walter A. Backofen. "Plastic instability and fracture in sheets stretched over rigid punches." *Asm Trans Q* 56.1 (1963):25-48.
- [19] Goodwin, G. M.: Application of strain analysis to sheet metal forming problems in the press shop, Society of Automotive Engineers (1968), No. 680093, 380-387.
- [20] Kaftanoglu, B. "Plastic analysis of flange wrinkling in axi symmetrical deep-drawing". *Proceedings of the Twenty-First International Machine Tool Design and Research Conference*. Macmillan Education UK, 1981.
- [21] Ramaekers, J. A. H., A. de Winter, and M. W. H. Kessels. "" Deep Drawability of a Round Cylindrical Cup." *IDDRG*. Vol. 94. 1994.
- [22] Cao, Jian, and M. C. Boyce. "A predictive tool for delaying wrinkling and tearing failures in sheet metal forming." *Journal of Engineering Materials and Technology* 119.4 (1997): 354-365.
- [23] Kawka, M., Olejnik, L., Rosochowski, A., Sunaga, H., & Makinouchi, A. (2001). "Simulation of wrinkling in sheet metal forming". *Journal of Materials Processing Technology*, 109(3), 283-289.
- [24] de Magalhães Correia, João Pedro, and Gérard Ferron. "Wrinkling predictions in the deep-drawing process of anisotropic metal sheets." *Journal of materials processing technology* 128.1 (2002): 178- 190.
- [25] Rees, D. W. A. "Factors influencing the FLD of automotive sheet metal." *Journal of materials processing technology* 118.1 (2001): 1-8.

- [26] Faraji, Ghader, Mahmud M. Mashhadi, and Ramin Hashemi. "Using the finite element method for achieving an extra high limiting drawing ratio (LDR) of 9 for cylindrical components." *CIRP Journal of Manufacturing Science and Technology* 3.4 (2010): 262-267.
- [27] Choubey, Ajay Kumar, Geeta Agnihotri, and C. Sasikumar. "Numerical Validation of Experimental Result in Deep-Drawing." *Materials Today: Proceedings* 2.4 (2015): 1951-1958.
- [28] Dieter, George Ellwood, and David J. Bacon. *Mechanical metallurgy*. Vol. 3. New York: McGraw-Hill, 1986.
- [29] Karl-Heinrich Grote and Erik K. Antonsson, "*Springer Handbook on Mechanical Engineering*": Springer Science and Business Media, LLC New York, 2008.
- [30] Altan, Taylan, and A. Erman Tekkaya, eds. *Sheet metal forming: fundamentals*. Asm International, 2012.
- [31] Erichsen, A. "A new test for thin sheets." *Stahl and Eisen* 34 (1914): 879-882.
- [32] Pomey, G.: Formability of thin sheet (in French). (Vol.1-3), Collection I.R.S.I.D.-O.T.U.A., Paris 1976.
- [33] Pomey, O.; Parniere, P.: Formability of thin sheet (in French), *Techniques de l'ingenieur* (1980), Nr.1, M 695,1-16, M 696,1-19.
- [34] Banabic, Dorel. *Formability of metallic materials: plastic anisotropy, formability testing, forming limits*. Springer Science & Business Media, 2000.
- [35] Fukui, S.: *Researches on the deep-drawing process*, Scientific Papers of the I. P. C. R. 34 (1939), 1422-1527.
- [36] Filip Lindberg, "Sheet metal forming simulations with FEM", *Master's Thesis in Engineering Physics*, 30 ECTS.